DEC 1958 29

REGISTERED NO. M. 3121

UNIVERSITY OF MICHIGAN
SEP 23 13
PHYSICS LIBRARY

PROCEEDINGS

OF THE

INDIAN ACADEMY OF SCIENCES

VOL. XLVIII] SECTION A [No. 1

JULY 1958

Price Rs. 2 or 3 Sh. Annual Subscription Rs. 18

Physics Library
QC
1
.I42

THE DIFFRACTION OF X-RAYS BY DIAMOND: PART III

By Sir C. V. Raman
(*Memoir No.* 109 *of the Raman Research Institute, Bangalore-6*)

Received May 7, 1958

1. Introduction

In the first part of the present memoir, it was shown from theoretical considerations of a very general nature that when X-radiations traverse a crystal, their passage could result in exciting vibrational transitions in the energy levels of the crystal and as a consequence of such excitation lead to a reflection of the incident X-rays by the lattice planes of the crystal with a change of frequency. The theory indicated it as an essential condition for such a process to occur that the vibrational transitions in question are effective as absorbers of infra-red radiation of the appropriate frequency. The phenomenon here envisaged is quantum-mechanical in its nature; in other words, vibrational transitions would be excited and would be accompanied by X-ray reflections of altered frequency even when the frequency of the vibrations is so high that they would not be thermally excited to any appreciable extent. However, considerations of a purely classical nature assist in elucidating the nature of the phenomenon and in deducing its observable features. The infra-red activity of a vibrational mode in a crystal arises because it involves a periodic displacement of the electronic clouds in the crystal with the same frequency; such a displacement would result in an oscillation of the stratifications of electron density which reflect the X-rays traversing the crystal and hence also to dynamic reflections of altered frequency.

Perhaps the most striking feature of the theory expounded in Part I is the connection which it indicates between the behaviour of a crystal in X-ray diffraction and the activity of the modes of its internal vibration in the absorption of infra-red radiation. The particular case of diamond is of special interest in this connection. For, as was shown in Part II of the memoir, theoretical considerations indicate that diamonds should be forthcoming in forms which differ in the inner symmetry of their electronic configuration and hence also in their infra-red behaviour. The detailed discussion showed that the diamonds of which the inner symmetry is octahedral would *not* exhibit dynamic X-ray reflections, whereas those diamonds of which the

symmetry is tetrahedral would exhibit such reflections. In other words, the case of diamond enables us to put the relation between X-ray diffraction and infra-red activity to a direct experimental test. Further, it was also shown in Part II of the memoir that in the case of diamond, we are concerned with three modes of vibration which are respectively parallel to the three cubic axes of crystal and hence variously inclined to the lattice-spacings in it. As a result, the dynamic reflections by these spacings differ both in their number and in their geometric configuration in a highly characteristic fashion. Thus, the application of the general theory to the particular case of diamond furnishes us with abundant material for comparison with the facts of experiment.

2. THE TETRAHEDRAL AND OCTAHEDRAL FORMS OF DIAMOND

Three diamonds employed in the present investigation are represented in Plate I. The first is a cleavage plate parallel to the (111) spacings of the crystal. The second is a flat tabular crystal in its natural form as a hexagonal plate with faces parallel to the (111) planes. The third is a thin facetted plate of diamond with its faces nearly parallel to the (111) planes. All three diamonds are perfectly colourless, without any visible cracks or inclusions in their interior and obviously of the highest quality. Nevertheless, the first two diamonds differ enormously in their physical behaviour from the third, as is apparent from a comparison of the photographs reproduced in the Plate. We proceed to explain how these photographs were obtained.

The photographs on the left-hand side were recorded by placing the diamond against a fluorescent screen. (This was a slab of lithium fluoride crystal impregnated with a little uranium oxide.) The λ 2537 radiation from a water cooled magnet-controlled mercury arc in quartz was isolated by a a monochromator and allowed to fall on the diamond and then on the $LiF\text{-}UO_2$ screen placed behind it, and the fluorescence excited in the latter was photographed from the rear. The photographs on the right-hand side of the Plate were obtained in a very simple manner. The diamond was placed between two crossed polaroids and photographed as seen through them against a bright source of light. It is seen from the photographs reproduced in Plate I that *the cleavage plate and the tabular crystal are both perfectly opaque to the* λ 2537 *radiations of the mercury arc and that they exhibit not a trace of birefringence, in other words that they are truly and perfectly isotropic crystals.* On the other hand, *the thin facetted plate is completely transparent to the* λ 2537 *radiations of the mercury arc, but it exhibits a feeble but nevertheless readily observable birefringence pattern with definite geometric features related in their orientation to the structure of the crystal.*

Diamond is, in effect, a giant macro-molecule of carbon. Hence a specimen of it which exhibits no detectable birefringence, in other words, is optically homogeneous, may, *prima facie*, be expected to make a close approach to the ideal state of crystal perfection. *Per contra*, a specimen of diamond—which exhibits over its entire area, a geometric pattern of birefringence however feeble it may be in intensity—must necessarily be regarded as very remote from such ideality. A striking confirmation of the correctness of these remarks is furnished by the results of a simple experimental test in which the diamonds figured in Plate I were used as X-ray spectrometers to resolve the $K\alpha_1$ and $K\alpha_2$ radiations from a copper target. The X-ray beam from the target diverged through a fine slit and fell on the diamond in an appropriate setting placed at a distance of 5 cm. from the slit. The surface reflection of the X-rays by the (111) planes of the crystal was recorded on a photographic film held at a distance of about 100 cm. The spectrograms recorded with the flat tabular diamond and by the facetted plate are reproduced as Fig. 1 (*a*) and 1 (*b*) respectively in Plate II. A very great difference between the two diamonds in regard to the degree of their crystal perfection is indicated by the difference in the two spectrograms. But the actual difference is even greater. For, the width of the $K\alpha_1$ and $K\alpha_2$ lines as recorded in Fig. 1 (*a*) in Plate II represents the natural spectral widths of these radiations and is therefore not a true measure of the crystal perfection of the tabular diamond. To obtain a true measure of that perfection, it is necessary to adopt a spectrographic technique in which two crystals of diamond are employed. The results of that technique are depicted in the series of spectrograms reproduced as Fig. 2 (*a*), (*b*), (*c*) and (*d*) of Plate II and in Figs. 1 (*a*), (*b*) and (*c*) of Plate X. We shall revert to the details of the technique and the significance of the results obtained with it in a subsequent section of the present paper.

Studies on the infra-red absorption spectra of diamond have established the fact that diamonds which are completely transparent to the λ 2537 radiations of the mercury arc in the ultra-violet are also completely transparent to infra-red radiations over the entire range of the characteristic frequencies of vibration of the structure of diamond ranging from 1332 cm.$^{-1}$ downwards to longer wavelengths. *Per contra*, the diamonds which are opaque to the λ 2537 radiations also exhibit a marked absorption over that entire range of infra-red wavelengths. It is thereby established that diamonds of the former kind possess an inner electronic configuration which has the full or octahedral symmetry of the cubic system, whereas the diamonds of the latter kind possess an electronic configuration which possesses the lower or tetrahedral symmetry of that system. The remarkable fact that diamonds with

a lower degree of symmetry are highly perfect crystals, while those with a higher degree of symmetry are highly imperfect receives a natural explanation on the basis of the theory of the structure of diamond expounded in Part II of the memoir. As there explained, the tetrahedral diamonds are those in which each dextro-carbon atom is linked to four lævo-carbon atoms and likewise each lævo-carbon atom is linked to four dextro-carbon atoms. *There is thus no physical difference between the two sub-species Td I and Td II* of the tetrahedral class of diamonds but only an interchange in the description of the two lattices which constitute the structure. On the other hand, the octahedral type of diamonds consists entirely of dextro-carbon atoms or entirely of lævo-carbon atoms; *the two sub-species Oh I and Oh II are therefore physically different*. These circumstances are clearly favourable for the Td diamonds exhibiting a high degree of homogeneity and for the Oh diamonds to be markedly heterogeneous in their texture. But there is another and a deeper consideration which has also to be borne in mind. When a dextro-carbon atom is linked to a lævo-carbon or *vice versa*, the two electrons shared between them describe their orbits about the valence direction in the same sense. On the other hand, when a dextro-carbon atom combines with a dextro-carbon atom or a lævo-carbon atom with a lævo-carbon atom, the shared electrons describe their orbits about the common valence direction in opposite senses. It would seem that a homogeneous structure extending through large volumes would be more likely to appear in the former case than in the latter.

It is appropriate at this stage to remark that it is the perfect diamonds belonging to the tetrahedral class that exhibit the phenomena of dynamic reflection of X-rays, while it is the imperfect diamonds of the octahedral type that do not show those phenomena. This is in agreement with the indications of the theory developed in Part II of the memoir. But it is necessary to demonstrate that the failure of the octahedral diamonds to exhibit dynamic reflections is not ascribable to their imperfection of structure, but is a consequence of their inactivity in infra-red absorption. We shall revert to this presently.

3. Dynamic X-Ray Reflections and Crystal Symmetry

Figure 1 in Plate III is a Laue photograph of a cleavage plate of diamond whose faces are parallel to the (111) planes of the crystal. The crystal was set exactly normal to a fine pencil of X-rays from a copper target. The picture shows perfect trigonal symmetry not only with regard to the ordinary or Laue reflections but equally also with regard to the dynamic reflections appearing in the vicinity of the hexagonal corners of the print adjacent to

the intense (111) Laue spots. Figure 2 in Plate III is a similar photograph taken in similar circumstances with a crystal of diamond which exhibits twinning of the spinel type. It will be seen that this pattern exhibits hexagonal symmetry in all its features, including especially the dynamic reflections which are seen at all the six corners of the hexagonal print. The fact clearly evident from Figs. 1 and 2 in Plate III that the dynamic X-ray reflections of diamond exhibit the symmetry of the crystal in the same manner and to the same extent as the static reflections is obviously of the highest significance. Taken in conjunction with the circumstance that the diamonds which exhibit the dynamic reflections are perfect and indeed—as will appear presently—are ideal crystals, it demonstrates the correctness of the view expressed by the author in the original publication of the year 1940 that these phenomena exhibited by diamond are fundamental in their nature and of the highest importance in relation to the theory of X-ray diffraction in crystals.

As already remarked earlier, the fact that the dynamic reflections are not manifested by the diamonds of octahedral symmetry is a confirmation of the theoretical ideas set out in Part I of the memoir. But the circumstance that these diamonds are imperfect tends to create some doubt in the matter. Very frequently, indeed, diamonds of this class give distorted Laue patterns. Hence a critical observer might be disposed to infer that it is this imperfection rather than the inactivity in infra-red absorption which is responsible for the non-appearance of the dynamic reflections. To dispel such an impression, it is necessary to investigate the matter with carefully selected material. The intensity of the birefringence exhibited by these diamonds is a measure of the imperfections in their structure. It is therefore desirable to select a specimen in which such birefringence is of extremely low intensity. The specimen illustrated in Figs. 3 (*a*) and 3 (*b*) in Plate I was found to be the best available in this respect. Even so, the mosaicity of its structure exhibits itself in a notable enhancement of the intensity of the Laue spots in its diffraction patterns. Such enhancement is particularly striking in the case of spots that are only feebly recorded with diamonds of the tetrahedral class. Even such a weak effect as the diffuse X-ray scattering due to thermal agitation is recorded with greatly enhanced intensity by this specimen. But there is no observable distortion of the Laue spots, and had the dynamic reflections been present, they would have been very striking features in the recorded patterns. Actually, not a trace of them is observable in Figs. 1 (*b*) and 1 (*d*) in Plate VIII which were recorded with this diamond in appropriate settings. For the sake of comparison, the patterns recorded with the tetrahedral diamond in identical settings are reproduced as Fig. 1 (*a*) and 1 (*c*) side by side with them in the same Plate VIII.

4. OBSERVABLE FEATURES OF THE DYNAMIC REFLECTIONS

The following special points are worthy of mention:

I. As the dynamic reflections by diamond are a consequence of the excitation by the incident X-rays of an infra-red vibration of high frequency, variations of temperature within wide limits should be entirely without effect either on the intensity or the sharpness of these reflections.

II. As a result of the crystal perfection of diamond, the ordinary reflections of monochromatic X-rays would demand a very precise setting of the crystal for their observation, on either side of which they would disappear completely. The dynamic reflections would coincide with the static reflections at the correct setting, but would not disappear when the setting is altered. Their intensity would however fall off rapidly as the crystal is moved away from the correct setting in their direction.

III. The dynamics of the excited vibration in diamond demands that the phase-waves which determine the direction in which the dynamic reflections appear are precisely normal to one or another of the cubic axes of the crystal. As a consequence, the reflections would be very sharply defined, being indeed in this respect almost comparable with the static reflections.

IV. By making observations of the directions in which the dynamic reflections appear, it is possible to determine the orientation of the phase-waves. The most suitable arrangement for such determination is to place the crystal so that one of the cubic axes lies in the plane of incidence of the X-rays on the (111) planes, and then to alter the setting in such manner that the plane of incidence does not change. The geometric law of dynamic reflection takes a very simple form in this case and a precise measurement of the orientation of the phase-waves becomes possible.

The various special features referred to above were all fully established by the observations made by the author and his collaborators in the months following the original publication of April 1940. Detailed reports of those studies appeared in the *Proceedings of the Indian Academy of Sciences* in the years 1940 and 1941. It would be superfluous here to traverse the same ground or to comment on the literature of a controversial nature published from other laboratories on the subject then and subsequently. To

make the present memoir complete, however, a series of photographs showing the dynamic reflections by the (111) planes, (220) planes, (311) planes and (400) planes of diamond in various settings are reproduced as Plates IV, V, VI, VII, VIII and IX accompanying the present paper. A comparison of the features noticed in this series of photographs with the theoretical diagrams given in Part II of the memoir will show how complete the agreement is between fact and theory.

5. Spectral Analysis of X-Ray Diffraction

We now return to a detailed description of the technique which enables a spectroscopic analysis to be made of the X-ray diffraction phenomena exhibited by diamond. The general nature of this technique to which a brief reference was made earlier will be evident from Fig. 1, text. A powerful source of X-rays from a copper target passes first through a wide slit and then

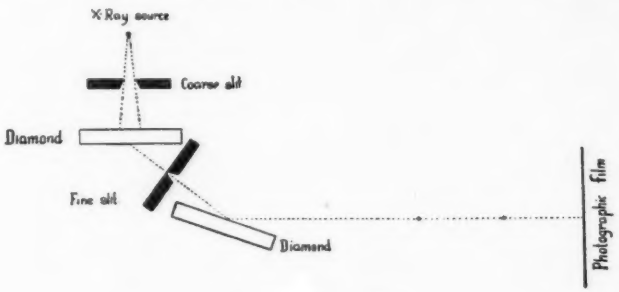

Fig. 1 (Text)

through the diamond under study. The rays *internally* diffracted by the (111) planes of this diamond are restricted by a fine slit through which they pass before they are incident on the surface of a second perfect diamond which functions as a spectrometer. The rays reflected *externally* by the second diamond are received and recorded on a photographic film placed at a distance of 100 cm. The actual technique consists in rotating the first diamond in steps through very small angles over a total range of a few minutes of arc. What is actually recorded on the photographic film is the spectrum of X-radiation in the narrow range between the $K\alpha_1$ and $K\alpha_2$ lines and perhaps a little more on either side of them.

The nature of the results obtained will be evident from a scrutiny of the series of spectrograms reproduced as Figs. 2 (*a*), (*b*), (*c*) and (*d*) in Plate II and the three others which appear as Fig. 1 (*a*), (*b*) and (*c*) in Plate X. The latter three have been enlarged so as to be readily comparable with the single

crystal spectrogram appearing as Fig. 1 (*a*) in Plate II. The most significant feature of the series of spectrograms is the appearance of an extremely sharp line which drifts in its position as the diamond is rotated. The spectral width of this sharp line is not more than about a tenth of the natural width of the $K\alpha_1$ or the $K\alpha_2$ radiations. It represents the super-monochromatic radiation manufactured by the first diamond from the incident white radiation by Laue reflections at the (111) stratifications. Its extreme sharpness reflects the extraordinary perfection of the diamond.

It will be seen that the relative intensities of the $K\alpha_1$ and $K\alpha_2$ lines differ enormously in the different spectrograms. That they persist over the whole range of settings of the diamond clearly shows that they represent the dynamic reflections of the $K\alpha_1$ and the $K\alpha_2$ radiations by the (111) planes of the first diamond. The static reflections of those radiations are recorded only at the precise settings at which those reflections are possible.

6. ACKNOWLEDGEMENT

The Laue patterns reproduced in Plates III, IV, V, VI, VII, VIII and IX, as well as the single crystal and double crystal X-ray spectra reproduced in Plates II and X accompanying this memoir were recorded in the X-ray Laboratory of the Raman Research Institute by the Assistant Director of the Institute, Professor A. Jayaraman, for whose valuable co-operation in the research the author of this memoir is greatly indebted. The gift to the Institute of a rotating target X-ray set by Sir Purushottamdas Thakurdas made the work possible.

7. SUMMARY

Studies on the crystal perfection of diamond by single-crystal and the double-crystal X-ray spectroscopic methods demonstrate that the non-birefringent diamonds which are infra-red active and possess only tetrahedral symmetry in their electronic configuration are extraordinarily perfect and are indeed ideal diamonds. It is these diamonds that exhibit the phenomena of dynamic reflection of X-rays. The detailed studies of the phenomena show that the experimental facts of the subject are completely in agreement with the results of the theory expounded in the first two parts of the memoir. The non-appearance of the dynamic X-ray reflections with the diamonds which have an octahedral symmetry of electronic configuration is shown to be consequential on these diamonds being inactive in the absorption of infra-red radiation.

FIG. 1 (*a*) (*b*)

FIG. 2 (*a*) (*b*)

FIG. 3 (*a*) (*b*)

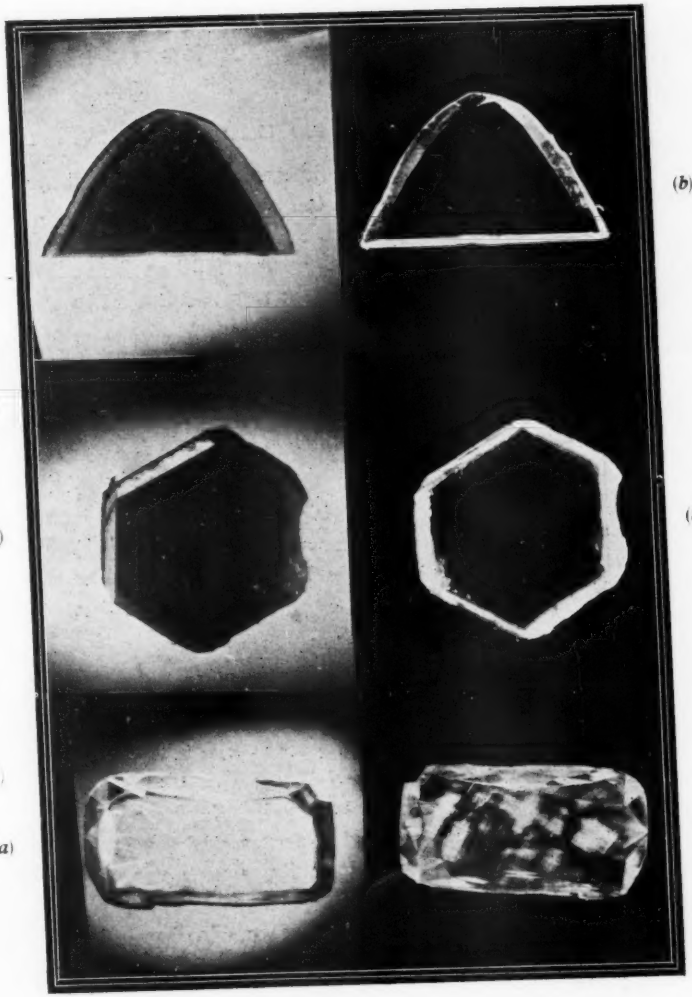

FIG. 1 (*a*) FIG. 1 (*b*)

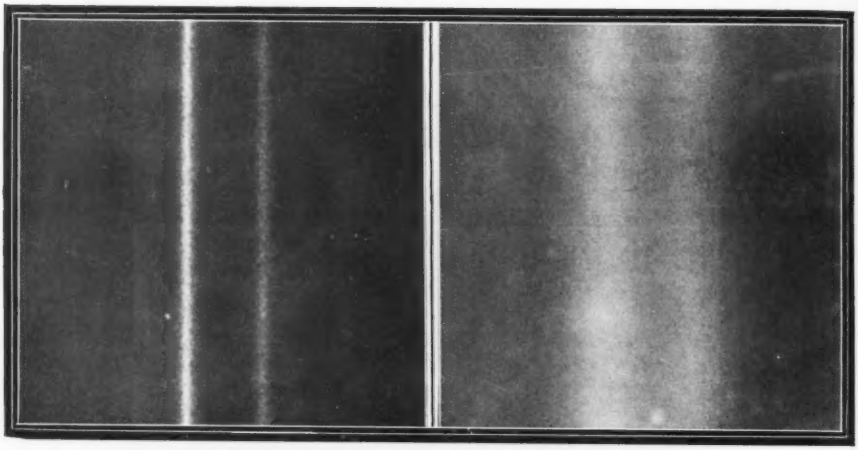

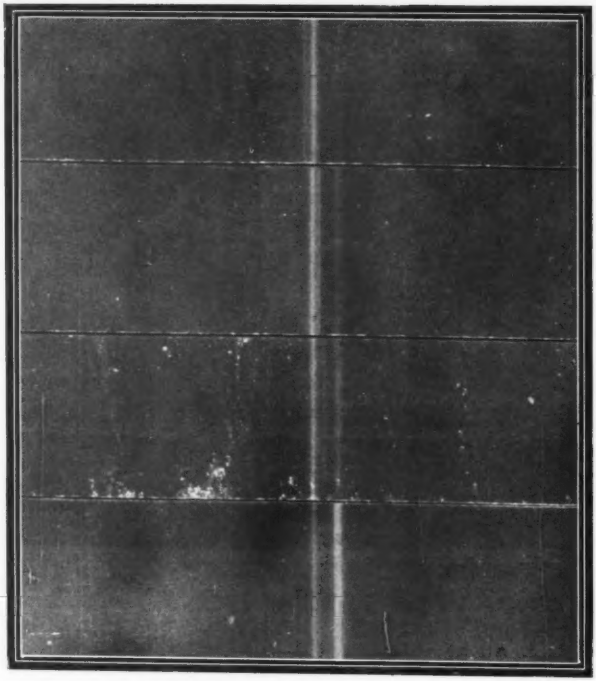

FIG. 2

FIG. 1

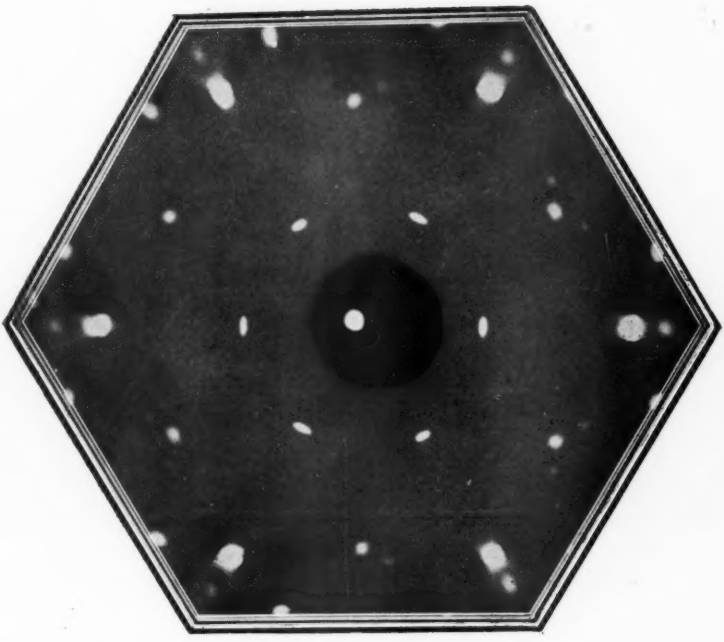

FIG. 2

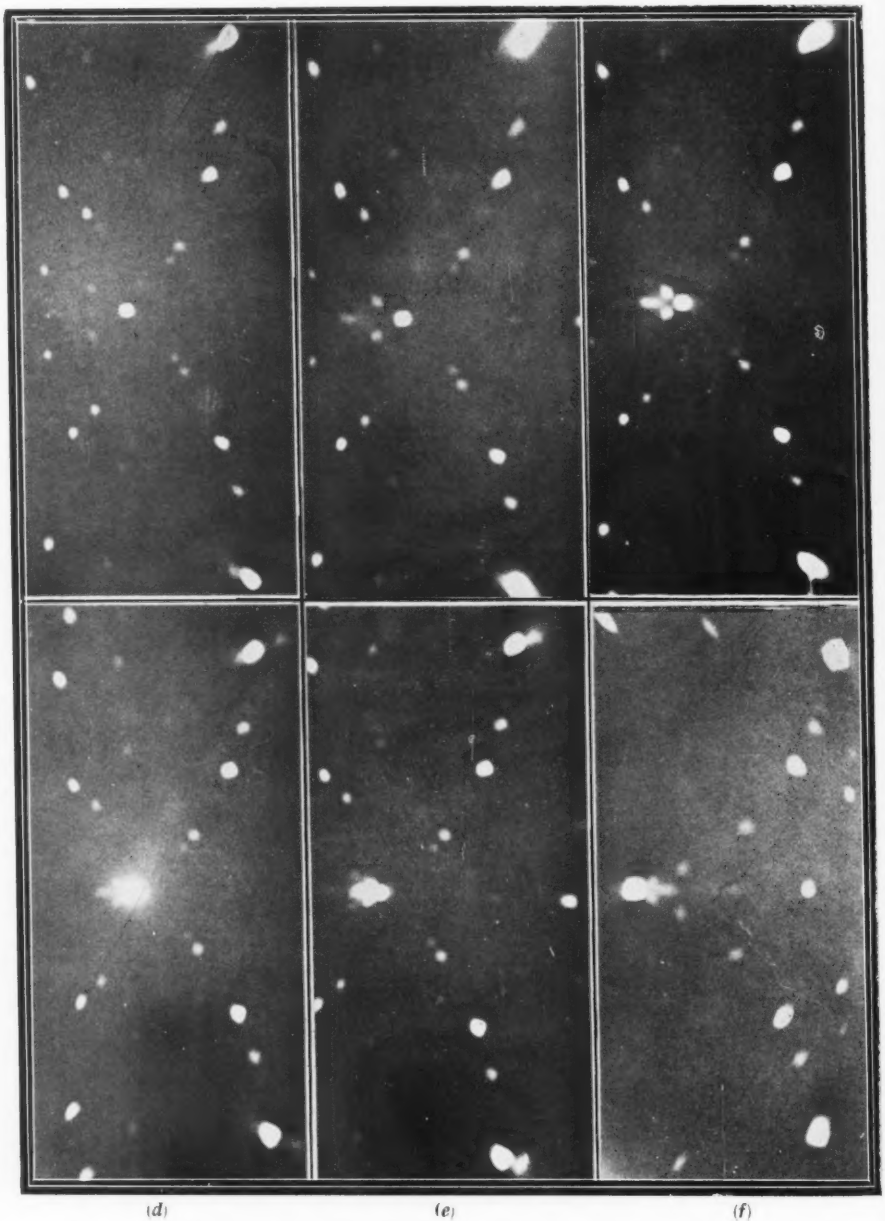

FIG. 1. Exhibiting the dynamic reflections by the (111) planes at various settings.

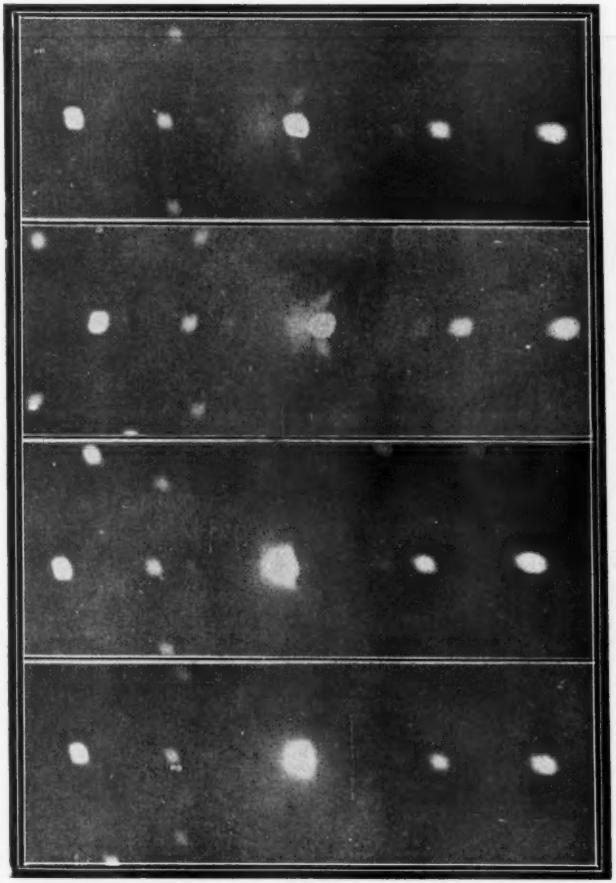

FIG. 1. Exhibiting the dynamic reflections by the (220) planes at various settings.

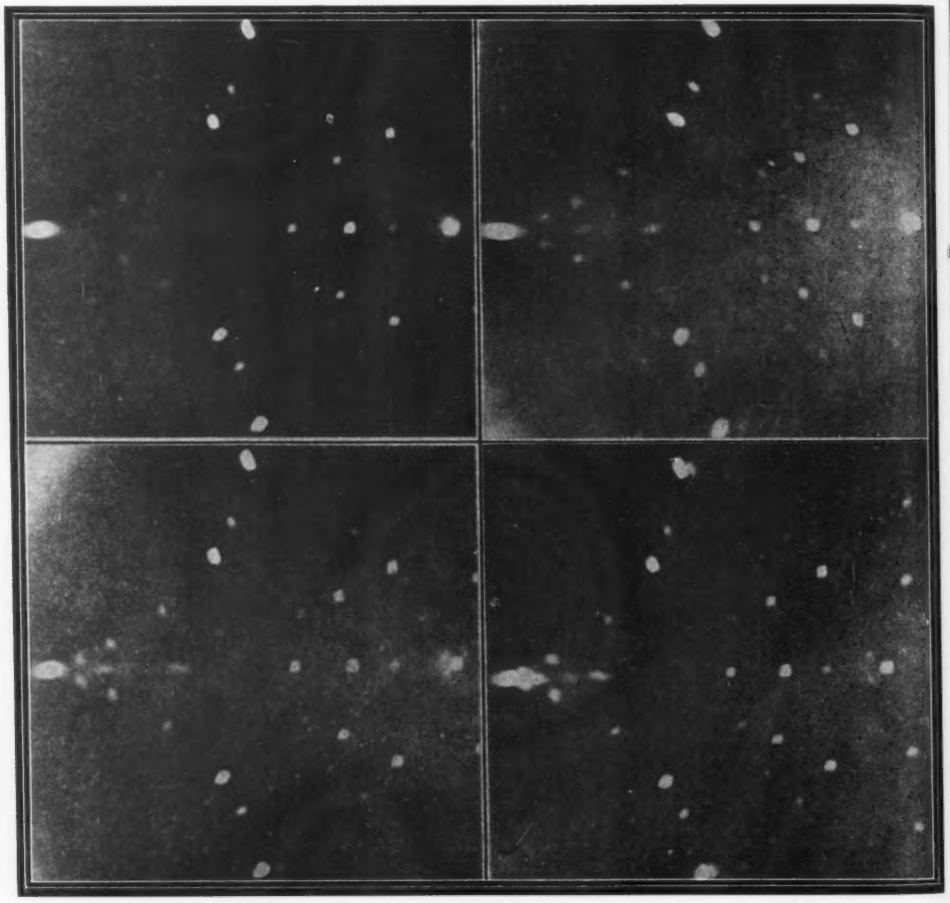

FIG. 1. Exhibiting the dynamic reflections by the (111) planes at the left and by the (113) planes at the right.

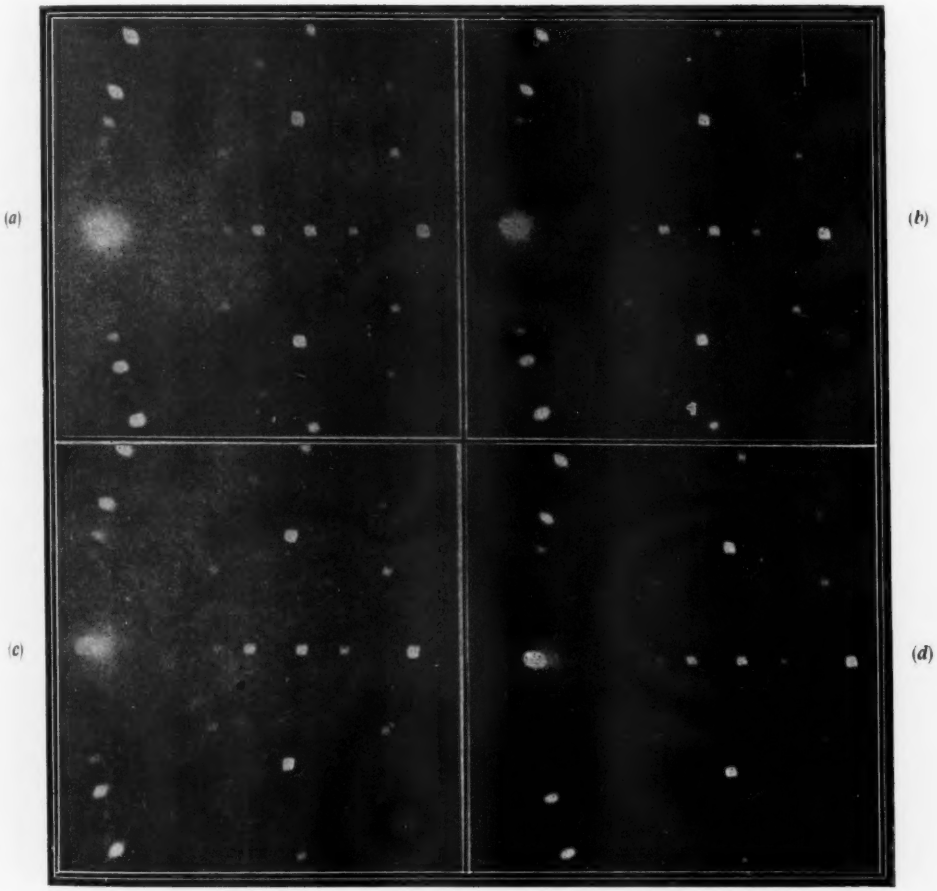

FIG. 1. Exhibiting the dynamic reflections by the (400) planes at the left.

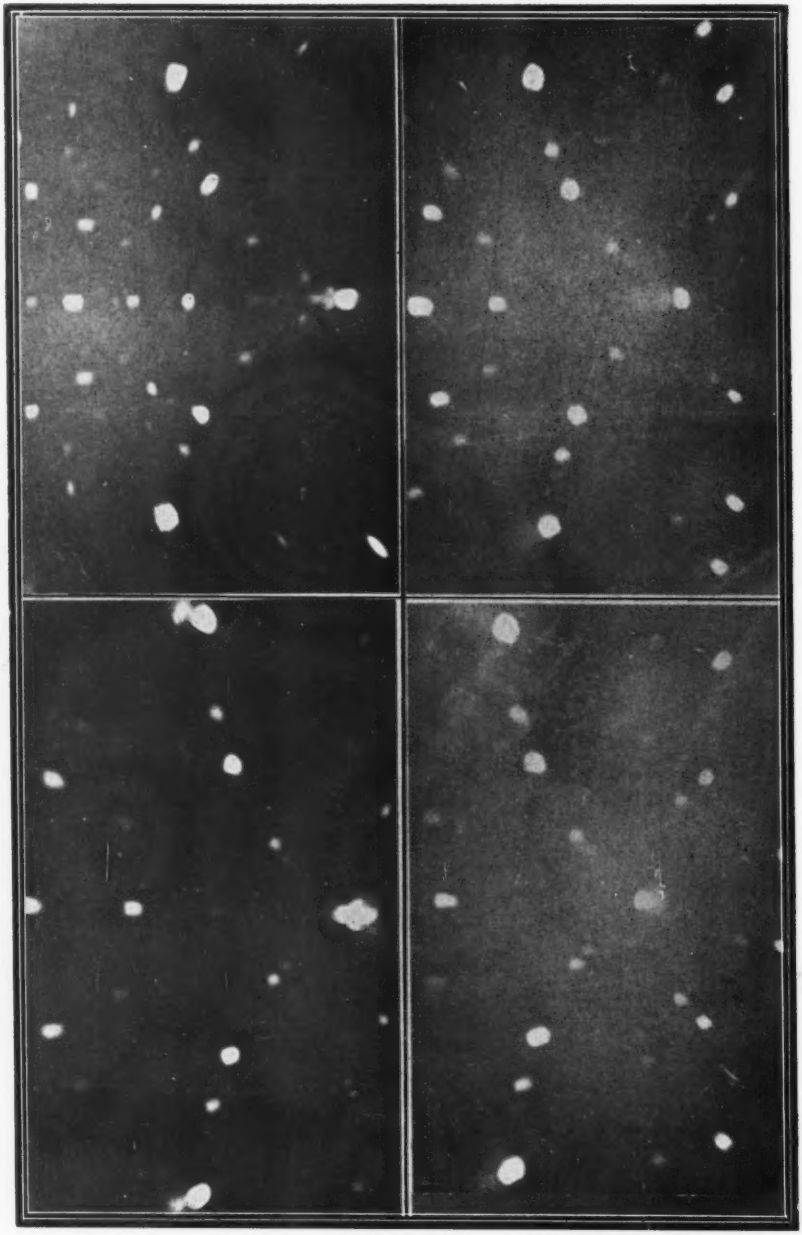

FIG. 1. Exhibiting the dynamic reflections by the (111) planes of tetrahedral diamond on the left and their absence with octahedral diamond on the right.

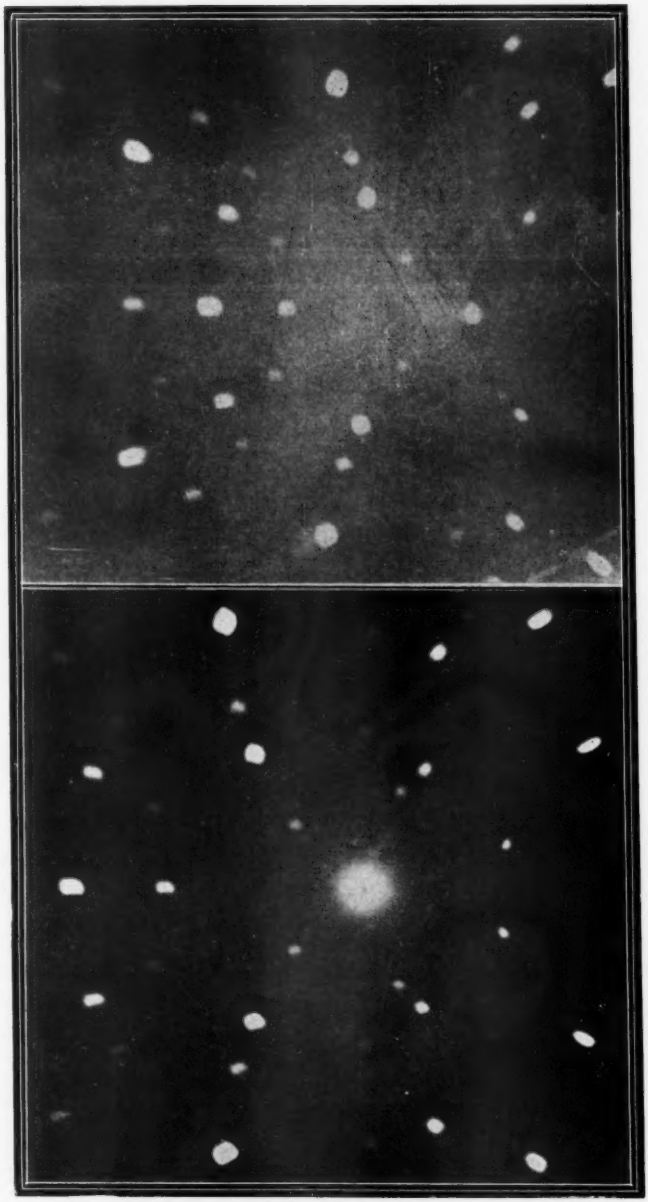

FIG. 1. Laue patterns of octahedral diamond showing intense reflection by the (111) planes at different settings.

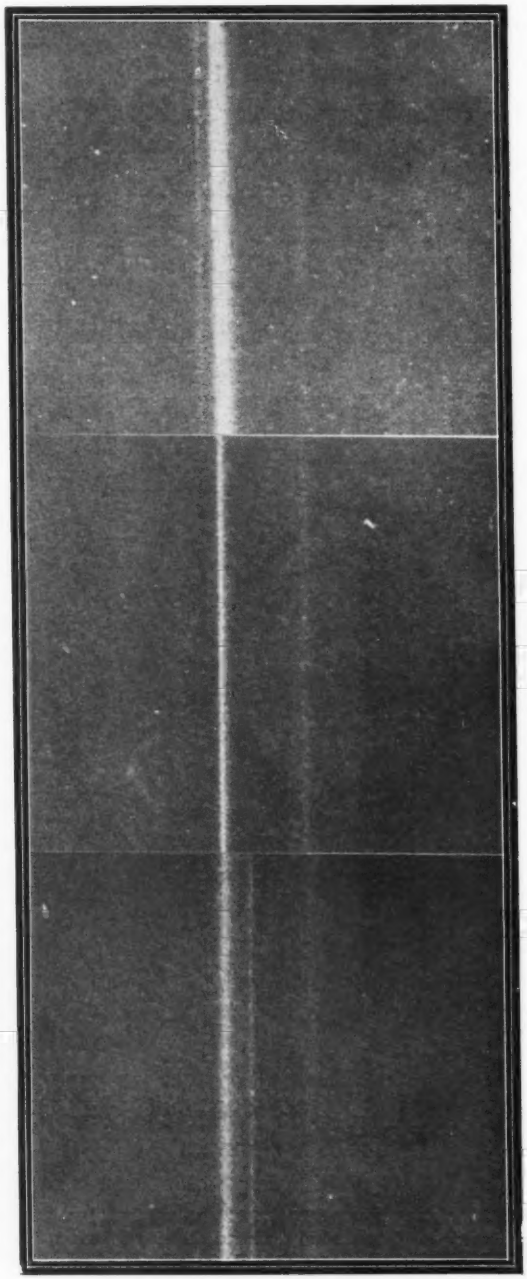

FIG. 1. For explanation, see text.

CLINOHUMITE SAUSAR SERIES, BHANDARA DISTRICT, INDIA

By T. N. Muthuswami, F.A.Sc.

(*Department of Applied Geology, University of Saugar*)

Received May 3, 1958

Introduction

This paper gives a mineralogical account of the humite mineral, clinohumite occurring in the dolomitic marbles of the Bichua stage of the Sausar series. This series—a member of the Archæan rocks of the Bhandara District, Madhya Pradesh, has been studied in great detail by Sir Lewis Fermor and the occurrence of the mineral has been reported by him (1921). However, so far there has not been any detailed study of any humite mineral occurring in India. The dolomitic marble specimens with the humite mineral were kindly made available by Dr. W. D. West from the collections he made with his student Mr. Manjrekar. The exact location is near Baoli, on the Bhawanthari river, about ten miles north-east of Deolapar.

Geological Setting

The Archæan terrane has been subjected to intense folding. It is in this classic ground that West (1926) has recognised nappe structure. The regional metamorphism is obviously connected with the folding movements of the originally horizontal sediments. The associated granites and injection gneisses are a natural accompaniment of folding. The impure dolomitic rocks have been metamorphosed to schists with anthophyllite and cordierite and the pure limestones to marbles with forsterite. In this regenerative process, the pneumatolytic effect of fluorine, that usually accompanies acid intrusives, is observed in the partial and complete conversion of forsterite to humite minerals.

The marble is white to greyish white, equigranular showing no well defined foliation, with calcite, diopside forsterite, the humite mineral, phlogopite, tremolite and spinel. Weathered rocks show the harder minerals in relief, calcite and phlogopite having been leached away. The humite mineral occurs in isolated grains or aggregates, giving rise to a streaky or banded

character to the rock. Lenticular concentrations, with insets of blue spinel are fairly common.

MINERALOGY

Clinohumite is one of the four members of the humite group of minerals. The designation humite mineral refers to any one of the four minerals. The humites are neo-silicates of magnesium containing hydroxyl and fluorine. The general formula is $Mg(OH, F)_2$—nMg_2SiO_4, where n may be 1, 2, 3 or 4, as shown below. Taylor and West (1928, 1929) have determined by X-ray studies, the structure of the humite minerals. They are made of interleaved slabs of $Mg(OH, F)_2$ and Mg_2SiO_4. The arrangement of the slabs is as follows: In norbergite n being 1, one slab of forsterite (Mg_2SiO_4) is interleaved with one of $Mg(OH, F)_2$; in chondrodite n equals 2, resulting in two slabs of forsterite following one of $Mg(OH, F)_2$; n is 3 in humite and 4 in clinohumite; hence every fourth slab in the former, and every fifth one in the latter, is forsterite.

It is a common feature of the humite minerals to show a diadochical replacement of Mg^{2+} by Fe^{2+} and Mn^{2+}; also a part of OH^- by F^-. The ionic radii of Mg^{2+}, Fe^{2+} and Mn^{2+} are 0·78 Å, 0·83 Å and 0·91 Å respectively. No complete hydroxyl end member, corresponding to brucite, $Mg(OH)_2$ seems to be present. Humite synthesis (1955), using hydrothermal techniques has been achieved. The hydroxyl end member has not resulted. Fluorine and hydroxyl are in the proper relationship to each other, as far as ionic size and charge are concerned, and hence efficiently exchange one for the other. Studies of anion exchange of $(OH)^-$ by F^-, in silicate structures have been made by infra-red spectroscopy (1957) and these have confirmed the ionic substitution. If a complete replacement of OH^- by F^- results, the fluorine end member sellaite MgF_2 will result. But the structural pattern of the end member brucite $Mg(OH)_2$, will be of the cadmium iodide type, while that of sellaite MgF_2 will be of the rutile type.

The slabs are arranged parallel to the basal pinacoid (1892, 1951); however some mineralogists take the arrangement as parallel to the ā pinacoid (1944, 1953); ă and b are essentially constant in absolute length. Since the slabs are packed in the direction of crystallographic c-axis, the length of this axis changes in a regular way, and is proportional to the number of Mg atoms in the mineral formula, which are 3, 5, 7 and 9.

The crystallographic and other data are given in Table I.

METHODS OF STUDY

The humite mineral was separated from dolomitic marble. The rock was crushed and ground to pass through sixty mesh. Grains in lots of

TABLE I

Crystallographic Data—Humite Minerals

Mineral	Crystal System and space-group	Slabs parallel to 001 Axial ratio and β				Value of c' in terms of 0·6287	Unit cell content		Stoichiometric ratio	
		a	b	c	β		$Mg(OH, F)_2$	$(Mg, Fe)_2SiO_4$	$Mg(OH, F)_2$	$(Mg, Fe)_2SiO_4$
Norbergite ..	Orthorhombic Phnm	1·0803	1	1·887	..	3 c	4	4	1	1
Chondrodite ..	Monoclinic $P2_1/c$	1·0663	1	3·1447	109°2′	5 c	2	4	1	2
Humite ..	Orthorhombic Phnm	1·0802	1	4·4033	..	7 c	4	12	1	3
Clinohumite ..	Monoclinic $P2_1/c$	1·0803	1	5·6588	100°50′	9 c	2	8	1	4

3–5 were examined under the microscope; the strong pleochroism brought out vividly the contrast between clinohumite and any other foreign grain or impurity. Grain after grain was thus picked out for chemical analysis and X-ray powder pattern. The method, though laborious eliminated all foreign material excepting pigments. Sahama has advocated a preliminary X-ray analysis, to ensure the purity of the sample under study. Sahama who kindly gave his authoritative opinion on the mineral wrote* "The powder pattern is good, and I could not detect any other humite mineral with certainty. It is possible that a very small quantity of humite is admixed with the clinohumite sample. If present, the amount of humite is, however, extremely small, and as a matter of fact, I doubt its presence."

OPTICAL DETERMINATION

The refractive indices were determined by the immersion method. Grains were selected from microsections, some showing maximum interference colours to determine α and γ; grains which under convergent light showed one isogyre splitting the field were selected for determining β. The cover slips were then removed by immersing the slides in xylol. The selected grains were transferred to separate slides, those showing maximum interference colours being kept separate, from those required to determine β.

The same grain was used to determine α and γ. Repeated washings by xylol and distilled water eliminated any trace of the liquid used. After careful wash the grain was removed to another slide by a match stick. Independent determinations were also made on individual grains. Grains so picked out from microsections bring out the Beckeline effect clearly, because of their being flat. The method though tedious is found very satisfactory to ensure good results. The R.I. of the liquid was immediately determined by the Billingham and Stanley refracto-meter.

SPECIFIC GRAVITY

The Specific Gravity was determined by a pyknometer and corrected to 20° C.

CHEMICAL ANALYSIS

This was kindly undertaken by Jun Ito of the Mineralogy Department of the Harward University (Mass). Fluorine value was obtained by H_2O_2 and TiO_2 method and also by semiquantitative spectroscopic analysis for CaF band.

---

* Personal communication.

TABLE II

Composition of Clinohumite

	Weight per cent.	Mol. ratio	Ratio O, OH, F atoms	Ratio Metal atoms	Basis 18 (O, OH, F)		Type formula clinohumite	Ratio ions		Electrical charges +	Electrical charges −
	(1)	(2)	(3)	(4)	(5)		(6)	(7)			
					(4)×6·34						
SiO_2 ..	37·18	0·6187	1·2374	0·6187	3·9226	3·92	4	Si^{4+}	3·9226	15·6900	..
Al_2O_3 ..	..	..	..	..	..			..		..	..
Fe_2O_3 ..	0·49	0·00306	0·0092	0·0061	3·0376			Fe^{3+}	0·0376	0·1128	..
FeO ..	2·24	0·0312	0·0312	0·0312	0·1978			Fe^{2+}	0·1978	0·3956	..
MnO ..	0·04	0·0005	0·0005	0·0005	0·0033	9·13	9	Mn	0·0032	0·0064	..
MgO ..	55·09	1·3663	1·3663	1·3663	8·6623			Mg	8·6623	16·3246	..
TiO_2 ..	2·92	0·0365	0·0730	0·0365	0·2314			Ti^{4+}	0·2314	0·9256	..
H_2O^+	1·30	0·0721	0·0721	(OH)0·1442	0·9142	1·23	2	OH^{1-}	0·9142	..	0·9142
F ..	0·95	0·0500	0·0500	0·0500	0·3170			F^{1-}	0·3170	..	0·3170
H_2O^-	0·25	..	..	..	..			O^{2-}	16·7688	..	33·4376
	100·46	..	2·8397	..	..		..		..	33·4550	34·6688
Less O for F	0·40										
	100·06										

(Multiplication factor to build 18 (O, OH, F) atoms in unit cell $18 \div 2·84 = 6·34$). Analyst: Jun Ito.

TABLE III

Clinohumites

Chemical Analysis with Atomic Proportions

	1	2	3	4	5	6	7	8	9	10	11	12	13	14	15
SiO_2	37·18	36·53	37·12	35·86	38·03	37·78	37·42	36·83	36·24	37·97	37·65	37·70	37·53	37·50	37·65
Al_2O_3	..	0·22	0·77	..	..	..	..	0·07	0·37	..	..	0·06	0·06	..	..
Fe_2O_3	0·49	0·56	0·32	0·22	..	..	0·46	0·42	4·69	..	..	..	..	..	..
FeO	2·24	5·04	3·44	14·25	4·83	5·64	1·27	4·90	6·20	1·12	1·29	2·51	1·57	3·84	3·41
MnO	0·04	0·34	0·15	1·19	..	..	0·10	0·28	0·30	..	0·44	0·03	1·39	0·23	0·50
MgO	55·09	54·16	54·85	44·66	54·00	53·05	56·32	51·53	46·05	56·60	55·00	54·10	53·76	52·55	51·74
TiO_2	2·92	0·26	1·48	0·06	..	..	1·14	1·92	5·20	0·68	1·00	2·52	2·96	3·96	5·40
H_2O^+	1·30	1·52	0·88	1·58	1·94	1·33	0·56	3·04	1·23	2·20	2·25	2·56	1·82	1·76	1·57
F ..	0·95	2·74	1·70	4·16	2·06	3·58	5·04	0·03	..	0·93	0·90	0·08	0·86	0·68	0·06
H_2O^-	0·25	0·04	..	..	..	..	..	0·12	..	..	..	..	..	..	..
Cl	..	..	..	..	..	..	..	..	..	..	..	0·16	..	0·20	0·20
CO_2	..	..	..	..	..	..	..	..	..	0·20	0·66	..	..	..	..
CaO	..	..	..	Tr.	..	..	..	..	..	0·30	0·85	0·13	0·76	..	0·10
K_2O	..	..	..	0·15	..	..	..	..	..	..	..	..	..	..	..
Na_2O	..	..	..	0·29	..	..	..	0·12	..	..	..	..	..	..	..
Total	100·46	100·41	100·71	102·42	100·86	101·38	102·31	99·26	100·28	100·00	100·04	99·85	100·71	100·72	100·63
Less O for F	0·40	1·15	0·72	1·75	0·86	1·50	2·12	..	..	0·43	0·38	0·07	0·36	0·33	0·08
Total	100·06	99·26	99·99	100·67	100·0	99·88	100·19	99·26	100·28	99·57	99·66	99·78	100·35	100·39	100·55

							99·26	100·28	99·57	99·66	99·78	100·35	100·39	100·55	

TABLE III (*Contd.*)

Atomic Proportions on Basis of 18 (O, OH, F) Atoms

	1	2	3	4	5	6	7	8	9	10	11	12	13	14	15
Si ..	3·92	3·79	3·90	3·80	3·94	3·89	3·74	3·94	3·97	3·94	3·97	3·98	3·95	3·95	4·00
Al ..	..	0·027	0·090	..	..	..	..	0·007	0·047	..	..	0·008	0·008	..	..
Fe^{3+}	0·038	0·044	0·025	0·018	..	..	0·035	0·034	0·385	..	..	..	..	..	..
Fe^{2+}	0·198	0·436	0·302	1·262	0·419	0·485	0·106	0·438	0·568	0·097	0·114	0·221	0·138	0·338	0·301
Mn	0·003	0·030	0·013	0·104	..	..	0·008	0·025	0·028	..	0·039	0·002	0·124	0·020	0·045
Mg ..	8·662	8·374	8·592	7·047	8·348	8·130	8·398	8·205	7·513	8·751	8·646	8·507	8·433	8·262	8·202
Ti ..	0·231	0·022	0·117	0·005	..	..	0·086	0·154	0·428	0·053	0·079	0·200	0·234	0·314	0·864
OH	0·914	1·053	0·616	1·115	1·341	0·912	0·373	2·166	0·90	1·524	1·582	1·801	1·276	1·239	1·114
F ..	0·317	0·900	0·565	1·393	0·675	1·164	1·594	1·010	..	0·305	0·300	0·027	0·287	0·227	0·020
	9·13	8·93	9·14	8·44	8·77	8·62	8·63	8·86	8·97	8·90	8·88	8·94	8·94	8·93	9·41
	1·23	1·95	1·18	2·51	2·02	2·08	1·98	2·18	0·90	1·83	1·88	1·83	1·56	1·47	1·13

X-RAY DATA

The powder diffractometer pattern of the sample was taken by Sahama with a Norolco diffractometer. A comparison with the pattern of his standard material (No. 865 + 9) Hameenkyla confirmed the identification. The data for the glancing angles 2θ, d spacings and intensities of the Sausar series mineral, and Sahama's standard were kindly given by R. Natarajan of Harward University.

OPTIC AXIAL ANGLE

The determinations of 2V were made on the universal stage by direct rotation from one optic axis to another, as this is decidedly the best method to ensure accuracy. The optic axes positions are read on the outer east-west axis, for two settings of the readings, 90 degrees apart. The two readings for each axis are averaged. The difference between the two averages is recorded as 2V, after necessary corrections. This procedure compensates for inaccuracies in the optic plane setting.

BIREFRINGENCE

The value was determined by Berek compensator.

The structural pattern of dehydrated clinohumite $MgF_2 . 4Mg_2SiO_4$ has a basis of 16 O ions and 2 F ions or 17 O ions. The substitution of OH, by F does not alter the relation of Mg to Si-ions. The pure OH mineral has the composition $Mg_9Si_4O_{16}(OH)_2$. The sum of the charges on the MgSi ions is 34 to balance the 17 O ions. Hence the ratio of Mg to Si for clinohumite, and similarly for any other humite mineral will be constant. For clinohumite this ratio is 9 to 4. For the mineral under study this ratio is 9·13–3·92, well within the results of analytical errors.

Si: (O_{Ti}, OH, F) RATIO

Ti^{4+} is usually considered to replace Si^{4+}. Geochemically, this replacement has been considered to be the most important one in silicates containing titanium. Kunitz (1936), as a result of intensive investigation considered that Ti–Si diadochy was common in garnets, amphiboles and micas. According to the recent trend of opinion in crystal chemistry, this mode of replacement is considered very limited because of the differences in the atomic radii of Si^{4+} (0·39 Å) and Ti^{4+} (0·64 Å). Ti^{3+} and Ti^{4+} favour substitution of Al^{3+} (0·67 Å) and Mg^{2+} (0·78 Å) in the structures. If then Ti^{3+} ions (0·69 Å) substitute Mg^{2+} (0·78 Å) of the brucite-sellaite slab, one should expect a similar substitution of the Mg^{2+} ions of the forsterite slabs

also of the humite mineral. However, there are evidences to indicate that the Ti–Mg diadochy is a restricted one confined to the brucite-sellaite slabs only. Firstly analysis of forsterite picked out from dolomitic marbles containing the humite mineral, shows an insignificant content of titanium, as recorded in the forsterite analysis from Ojama, Finland (1953). Secondly, as pointed out by Borneman-Starynkevitch and Mjasnikov (1950), analytical results agree better with the structural formula if titanium is not added to the magnesium of the forsterite slab. Thirdly, the crystal structure of TiO_2 is similar to that of MgF_2; OH, when present, is not so far known to alter the structure. Perhaps the water of the cell content, in the brucite-sellaite slab, acts as a catalyst to initiate and aid the atomic substitution.

If this assumption of restricted diadochy of Ti–Mg in the brucite-sellaite slab is accepted, this would also involve a substitution of F in the slab by the O associated with Ti. Thus F will decrease as O and OH increase; However, the atomic ratio of any humite mineral—Si to (O_{Ti}, OH, F) will be constant and prove a diagnostic feature. For clinohumite the average ratio of thirteen selected analyses is given as 8 : 4·20 (Table IV), while the theoretical value should be 8 : 4. The minimum for O_{Ti}, OH, F is 2·9 and the maximum is 5·3. In the clinohumite (this paper) this value is 3·45, well within the limits. In this connection, it may not be inappropriate to point out that the determination of H_2O is a difficult problem in mineral analysis, and particularly so in the humite minerals. Water is tenaciously adsorbed in the cell structure. It also contains 89 per cent. of oxygen—a percentage much higher than any other oxide; this will inevitably result in errors in the oxygen atoms per unit cell even for a small percentage error in the analysis. Further water has a low molecular weight compared to others, which will also affect the computation.

O_{Ti}, OH, F Ratio

The next mode of interpreting the analysis is to find out if an increase of O_{Ti} goes with a decrease of F, with the three variables O_{Ti}, OH and F. Sahama has plotted in a triangular diagram, the three anions of selected analyses (Fig. 1). There are eleven plots in the diagram of Sahama. That marked (1) is the O_{Ti}, OH, F ratio of the mineral under study of values 27, 54 and 19 (Table IV) respectively. Admittedly taken as a whole, the figure does not bring out the relationship it is intended to convey. Out of the twelve plots, seven are scattered far down below to formulate authoritatively that an increase in O_{Ti}, results in a decrease of F. But neglecting the plots with low titanium content, a tendency in the direction expected is observed. The real difficulty seems to be this. Crystal lattices attain the

TABLE IV

	1	2	3	4	5	6	7	8	9	10	11	12	13	14	15	16
	Atomic ratio of silicon. Basis 8 to (O_{Ti}, OH and F)															
O_{Ti}+OH+F ..	3·45	4·13	2·9	5·3	..	..	4·57	5·08	3·53	3·93	4·11	4·48	4·11	4·23	3·99	..
	Average ratio Si to (O,OH, F)=8 : 4·20															
	O_{Ti}, OH, F—per cent.															
%																
O_{Ti} ..	27	2	17	0·4	..	..	8	12	49	5	8	18	23	30	43	..
OH ..	54	53	43	44·1	..	..	17	87	51	79	77	81	63	59	56	..
F ..	19	45	40	55·5	..	..	75	1	..	16	15	1	14	11	1	..
	Optical values															
α ..	1·638	1·629	1·633	1·652	1·625	1·632	1·628	1·664	1·691							1·655
β ..	1·650	1·641	1·643	1·663	1·638	1·644	1·642	1·673	1·700							1·678
γ ..	1·670	1·662	1·674	..	1·653	1·664	..	1·698	1·724	Optical data not reported						1·700
$\sqrt[3]{\alpha\beta\gamma}$ ..	1·652	1·644	1·650	..	1·639	1·647	..	1·678	1·704							1·677
$2V\gamma$ ..	76°	73°	73°	76°27′	near 90°	74°	..	62°	58°							near 90°
Extinction $\alpha \wedge 001$	9°	11°	9°	12–15°	..	..	..	..	..							..
	Specific Gravity															
Specific Gravity	3·23	3·26	3·215	3·350	3·184 3·222	3·219 3·258	3·170	..	..	3·157	3·162	3·181	3·216	3·231	3·253	..

Index for the Tables III and IV—

1. This Paper—Sausar Series, India.
2. Th. G. Sahama (1953) Hameenkyla, Finland.
3. Th. G. Sahama (1953) Ojama, Lohja, Finland.
4. Sjogren (1894), Larsen (1953) } Nordmark.
5. Penfield and Howe (1894), Larsen (1928) } Vesuvius Brush collection 2,064.
6. Penfield and Howe (1894), Larsen (1928) } Vesuvius Yale 4,143.
7. Walker and Parsons (1927), Larsen (1928) } Chaffey's Lake, Ontario.
8. Zambonini (1919), Larsen (1928) } Piedmont.
9. Quervain (1938) Alpe, Canciano.
10–15. Borneman Staryn-Kevitch and Mjasnikov Achmatovsk 1–6.
16. Lindberg, M. L., 1946, *Bull. Geol. Soc. Am.*, p. 1213.

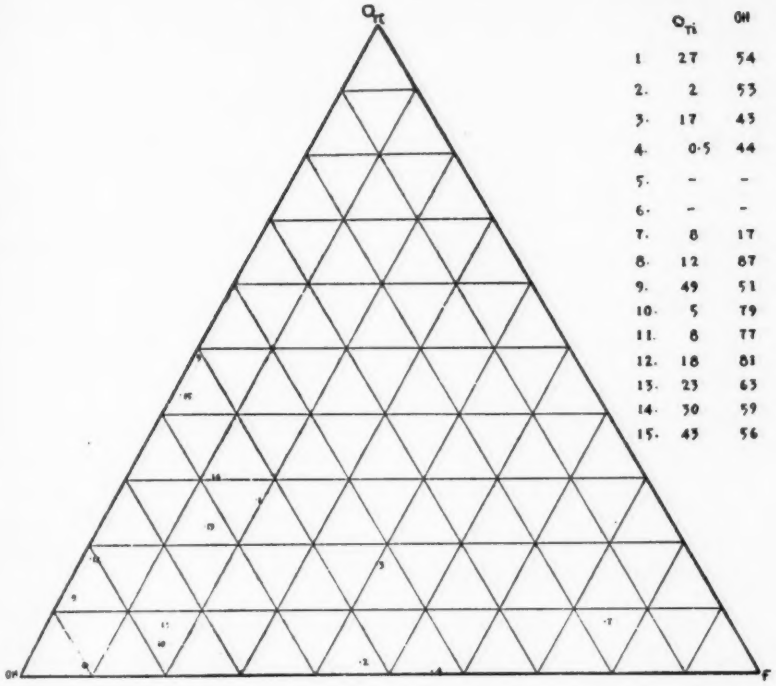

	O_{Ti}	OH	F
1.	27	54	19
2.	2	53	45
3.	17	43	40
4.	0·5	44	55·5
5.	–	–	–
6.	–	–	–
7.	8	17	75
8.	12	87	1
9.	49	51	–
10.	5	79	16
11.	8	77	15
12.	18	81	1
13.	23	63	14
14.	30	59	11
15.	43	56	1

FIG. 1. Clinohumite (O_{Ti}, OH, F) ratio.

ideal type only at the absolute zero of temperature. At all other temperatures, thermal vibrations produce defects either in the form of holes, or in some atoms not taking their legitimate positions. In the increased temperature of metamorphism the defects perhaps become much greater.

PHYSICAL AND OPTICAL CHARACTERS

Physical Characters

Crystal form absent; subhedral, Colour—of shades of yellow, brown to dark brown often violetish in weathered specimens. Cleavage poor. H 5·5–6, fracture subconchoidal to conchoidal. Lustre vitreous. Specific Gravity 3·2.

Twinned on 001, simple and polysynthetic—the bands of varying width; cracks usually present.

16. Lindberg, M. L., 1940, *Bull. Geol. Soc. Am.*, p. 1213.
6. Penfield and Howe (1894) } Vesuvius Yale 4,143.
Larsen (1928) }

Optical Properties

Pleochroism	..	α = Golden yellow. β = Pale yellow. γ = Pale yellow.
Refractive indices	..	$\alpha = 1{\cdot}638$ $\beta = 1{\cdot}658$ } $\pm 0{\cdot}001$. $\gamma = 1{\cdot}670$
Birefringence	..	Strong with middle second order interference colours.
Double refraction	..	·032.
2V	..	76° (corrected for R.I. Segments).
Sign	..	Positive.

Extinction .. $\alpha \wedge 00I = 9°$; symmetrical on either side of the trace of the composition plane 00I, γ coinciding with the microscope axis. Random sections, orientated with the twinning line bisecting the angle 18–20°, between the extinction positions of α of two adjacent bands are noted. The adjacent lamellæ of such grains show equal illumination eight times on a complete rotation of the stage.

REFRACTIVE INDICES AND OPTIC AXIAL ANGLES

A reference to the refractive indices of 29 chondrodites (Table V), nine clinohumites (Table IV) and ten humites (Table VI) collected from literature indicates that there is considerable overlap in the R.I. values of α, β and γ. With reference to these three humite minerals, on the basis of the available data, it may be tentatively inferred that a humite mineral is chondrodite provided α is less than 1·607, or β less than 1·619 or γ less than 1·639. Also, if β is more than 1·655 or γ more than 1·675, it can be clinohumite. The identification of norbergite is best done by its optic axial angle $2V_\gamma = 44–50°$. Only eight values of $2V_\gamma$ are available for humite and eight for clinohumite. The range in the former is 65–84° while in the latter it is 58–90°. Out of the sixteen readings available for chondrodite the range is 70–90°.

OPTICAL PROPERTIES AND CHEMICAL COMPOSITION

The relation between the chemical composition and optical values for the humite mineral cannot be made out, as the available data are too scarce to draw a generalised conclusion. Further the refractive index is influenced by the chemical content of various constituents like FeO, MnO, TiO_2, F and H_2O. However, it may be mentioned that Thiele (1940) shows that

TABLE V

Chondrodite

Refractive Indices, 2V and Specific Gravity

	1	2	3	4	5	6	7	8	9	10	11	12	13	14
α ..	1·592	1·593	1·594	1·600	1·601	1·601	1·602	1·604	1·605	1·607	1·607	1·607	1·608	1·638
β ..	1·602	1·606	1·607	1·609	1·616	..	1·611	1·613	1·616	1·617	1·619	1·620	1·620	1·619
γ ..	1·621	1·622	1·619	1·628	1·638	1·637	1·630	1·633	1·636	1·639	1·639	1·643	1·642	1·640
	1·605													
$\sqrt[3]{\alpha\beta\gamma}$ ..		1·607	1·606	1·612	1·619	..	1·614	1·617	1·619	1·621	1·621	1·623	1·624	1·622
2Vγ ..	..	..	Lge	72°	..	85–90°	72°	72°	73°	80°	..	72°14′	74°	77°
Extinction ..	..	..	..	26°	28°56′	27°2′	26°	22°	..	28°	30°	26°25′	..	27°
Specific Gravity	..	..	..	3·177	3·227	..	3·191	3·161	3·168	3·260	..	..	3·252	3·217
									3·235				3·265	

	15	16	17	18	19	20	21	22	23	24	25	26	27	28
α ..	1·609	1·609	1·610	1·611	1·612	1·613	1·613	1·615	1·619	1·619	1·621	1·631	1·635	1·643
β ..	1·619	1·622	1·623	1·622	1·619	1·625	1·623	1·627	1·632	1·630	1·632	1·640	1·645	1·655
γ ..	1·641	1·643	1·643	1·641	1·641	1·643	1·643	1·646	1·653	1·650	1·655	1·657	1·663	1·670
$\sqrt[3]{\alpha\beta\gamma}$ ..	1·623	1·625	1·625	1·625	1·624	1·627	1·627	1·629	1·635	1·633	1·636	1·643	1·648	1·657
2Vγ ..	..	79°	74°	..	73°	72°	70°	75°	79°40′	71°	..	med	Lge	Lge
Extinction ..	..	31°	26°	27°	26°	26°34′	..	24°	27°30′	..	31°	..	26°	..
Specific Gravity	3·194	3·241	..	..	3·224	..	..	3·228	3·28	..	..	..	3·204	..
	3·215												3·231	

Index—

1, 11, 12, 21, 24 and 28, Winchell, A. N. and Winchell, H. (1951).

2, 3, 5, 6, 9, 13, 15, 18, 23, 25, 26 and 27, Larsen, E. S. (1928).

4, 7, 8, 10, 14, 16, 19, and 22, Sahama, Th. G. (1953).

17, Sadashiviah and Ghosh (1953).

20, Eckermann (1922), *Geol. For. Forh, Stockholm.*

TABLE VI

Humite

Refractive Indices, 2V and Specific Gravity

	1	2	3	4	5	6	7	8	9	10
α ..	1·607	1·607	1·621	1·621	1·623	1·624	1·625	1·632	1·641	1·643
β ..	1·619	1·623	1·627	1·629	1·634	1·633	1·635	1·643	1·649	1·653
γ ..	1·639	1·643	1·649	1·652	1·655	1·653	1·656	..	1·672	1·675
$\sqrt[3]{\alpha\beta\gamma}$ ..	1·622	1·624	1·632	..	..	..	1·639	..	..	1·657
2V ..	76°	84°	..	65°	69°	66°	70°	..	75°	68°
Specific Gravity	3·202	3·236	3·194 3·201	3·214	..	3·245	3·183 3·225	3·32	3·243	3·273

Index—

1, 2 and 10, Thiele (1940).

3, 7 and 8, Larsen, E. S. (1928).

4, 6 and 9, Sahama, Th. G. (1953).

5, Rankama (1938).

TABLE VII*

Chondrodite

No.	Vorkommen	Fe_2O_3	FeO	$Fe''+Fe'''$	n_m	Analyst
5	Warwick ..	..	2·64	2·87	1·619	Penfield
9	Mansjo ..	..	3·67	4·08	1·623	Eckermann
2	Mt. Somma ..	0·54	3·85	4·80	1·623	Thiele
10	Hermala ..	1·86	4·16	6·48	1·626	Jernefelt
3	Tilly Forster ..	0·63	5·34	6·59	1·628	Thiele
14	Brewster ..	..	5·91	6·66	1·628	Penfield
15	Ristienne ..	0·30	8·70	9·97	1·628	Rankama
16	Nordmarken ..	0·54	10·54	11·97	1·635	Mauzelius

* From Thiele, *Chemie der Erde*, 13, p. 73.

TABLE VIII

Clinohumite

Phillips Geiger Counter X-ray Spectrometer Cu/Ni-Ka

Powder pattern data						Diffractometer data					
1 Sahama's No. 865+9 Hameenkyla, Finland			2 This Paper—Sausar Series			3 Sahama's No. 865+9 Hameenkyla, Finland			4 This Paper—Sausar Series		
2θ	d	I	2θ	d	I	2θ	d	I	2θ	d	I
17·55	5·05	m	17·61	5·04	s	17·62*	5·02	s	17·70	5·01	s
19·89	4·46	w	20·03	4·43	m	19·96	4·44	w	20·00	4·44	w
22·95	3·88	w	23·00	3·86	w	22·96	3·86	w	23·05	3·87	w
24·02	3·70	ms	24·11	3·69	s	24·00	3·70	s	24·07	3·70	s
25·60	3·48	ms	25·62	3·47	m	25·50	3·48	w	25·61	3·48	w
..	..	..	..	..	..	25·80	3·44	w	25·87	3·44	w
26·50	3·36	w	26·58	3·35	vw	26·55	3·35	vw	26·62	3·35	w
27·50	3·34	ms	27·58	3·23	s	27·63	3·22	m	27·70	3·22	m
..	..	..	31·11	2·87	vw	30·58	2·91	vw	..	..	..
32·53	2·76	s	32·52	2·75	vs	32·33	2·76	s	32·39	2·76	vs
..	..	..	..	..	..	32·68	2·73	m	32·70	2·74	m
..	..	..	..	..	..	33·35	2·68	vw	33·45	2·68	w

34·35	2·61	m	34·53	2·60	w	34·38	2·60	w	34·45	2·60	m
35·34	2·54	m	35·28	2·53	vs	35·22*	2·54	s	35·30	2·54	m
35·94	2·50	m	35·84	2·50	vs	35·68	2·51	s	35·75	2·51	s
37·32	2·41	w	37·40	2·40	w	37·29	2·40	w	37·40	2·40	w
..	..	..	..	..	..	37·54	2·39	vw	37·64	2·39	m
38·16	2·36	w	38·15	2·36	w	38·07*	2·36	m	38·15	2·37	m
..	..	..	39·06	2·30	vw	38·98	2·30	vw	39·05	2·31	w
39·95	2·26	s	39·97	2·26	vs	39·77	2·26	s	39·87	2·26	s
..	..	..	42·13	2·14	vs	41·89	2·15	vw	..	..	..
52·41	1·75	s	52·45	1·745	vs	52·37	1·742	s	52·45	1·745	vs
..	..	..	52·95	1·728	vs	52·51	1·738	vs	52·60	1·740	vs
54·36	1·69	w	54·56	1·682	w	54·42	1·681	vw	54·48	1·680	w
56·45	1·63	w	..	..	..	56·49	1·624	vw	..	..	..
..	..	..	57·03	1·614	w	56·95	1·612	vw	57·05	1·610	w
60·13	1·54	w	60·35	1·534	w	60·02	1·537	vw	60·08	1·540	vw
..	..	..	..	..	..	62·20	1·488	vw	62·30	1·490	w
62·64	1·480	ms	62·82	1·479	s	62·61	1·479	m	62·78	1·480	w
66·83	1·400	m	67·14	1·394	m	66·84	1·398	vw	66·88	1·400	w
69·79	1·350	m	70·11	1·342	s	69·70	1·345	w	..	..	..

Courtesy of R. Natarajan, Harvard (Mass.).

Dr. Frondel, Harvard (Mass.).

Sahama (1953)
* Lines diagnostic.

R. Natarajan, Harvard (Mass.).

the mean refractive index of chondrodite increases with increase in Fe^{2+} and Fe^{3+}, as shown in Table VII reproduced from Thiele.

Extinction $\alpha \wedge$ 001

Though the determination of the refractive indices and optic axiatl angles are not useful in the specific identification of humite, chondrodite and clinohumite, the extinction value $\alpha \wedge$ 001 is a useful criterion. The recognition of the morphological feature (001) depends on the crystal being twinned on (001). If the orientation of the grain is such that if a tilt on the N.S. axis in the U stage preferably does not exceed 15°, γ being made to coincide with the mircoscope axis, the symmetrical extinction (1951) for the humite minerals is as follows:

Humite	..	0°.
Clinohumite	..	7–15°.
Titan clinohumite	..	20°.
Chondrodite	..	26–30°.

For the mineral under study, the extinction is 9°; indeed, grains with orientation exactly perpendicular to γ, giving symmetrical extinctions, without a need for investigation on the U stage, confirmed the correctness of the identification.

X-Ray Powder Data

In the absence therefore of twinning lamellæ, the specific determination of a humite mineral is practically impossible. The only method is to compare the X-ray powder pattern with a standard pattern of humite mineral. Here again the purity of the mineral for taking the standard should be rigidly ensured. Sahama's standard No. 865 + 9, of clinohumite Hameenkyla, Finland, serves the purpose of a standard.

Table VIII gives the X-ray data for glancing angles (2θ), d-spacings (d) and estimated intensities (I) of the lines for the Sausar series mineral and Sahama's standard. The patterns were obtained in both cases by Philips Geiger Counter X-ray spectrometer, using Cu-Kα radiation and nickel filter. The asterisks in the column 2θ are recommended as diagnostic of clinohumite by Sahama. The identification is well established.

ACKNOWLEDGEMENTS

By courtesy of Dr. W. D. West and his stimulating influence, the present writer was enabled to write this short paper. The chief object was to study and establish beyond doubt the identification of the humite mineral.

Prof. Th. G. Sahama was kind enough to confirm the identification of th mineral by X-ray investigation and comparison with his standard material (No. 865 + 9). Thanks are due to Mr. R. Natarajan and Dr. Frondel, Harvard University, for letting me have the X-ray data. The chemical analysis was done by Jun Ito of the Mineralogical Department, Harvard University (Mass.). Prof. Percy Quensel, Stockholm University, was so kind as to supply the chemical analytical data of some of the comparable humite minerals, which could not be easily located in India. The microphotographs were kindly prepared by Dr. West for publication.

The interest and help received from one and all, in writing this paper, is hereby gratefully acknowledged.

References

Berman, H. .. *Am. Min.*, 1937, **22**, 397.

Borneman-Staryn Kevitch, I. D. and Mjasnikov *Inst. Geol. Sci. Acad. U.S.S.R. Akad. Nauk. S.S.S.R.*, 1950, **71** (1), 137.

Dana, E. S. .. *A System of Mineralogy*, 1891.

Eckermann .. *Geol. For. Forh. Stockholm*, 1922, **44**, 203.

Fermor, L. L. .. *Rec. Geol. Surv. Ind.*, 1921, **53**, 21.

Goldschmidt, V. M. .. *Geochemistry*, Oxford, 1954.

Huang, W. T. .. *Am. Min.*, 1957, **42**, 686.

Larsen, E. S. .. *Ibid.*, 1928, **13**, 354.

Lindberg, M. L. .. *Bull. Geol. Soc. Am.*, 1946, **57**, 1213.

Narayanaswamy, S. and Malhotra, P. D. *Proc. 45th Ind. Sci. Cong.*, Part III, *Abstract*, 1958, p. 222.

De Quervain, F. .. *Schweiz. Min. Petr. Mitt. Bd*, 1938, **18**, 591.

—— and Friedlaender, C. .. *Chemismus Schweizerischer Geisteine—Beitrage zur Geologie der Schweiz. Geotechn. Serie* 20, *Leiferung.*

Rankama, Kalvero .. *C. R. Soc. Geol. Finlande Bull. Comm. Geol. Finlande*, 1938.

———— .. *Am. Min.*, 1947, **32**, 146.

—— and Sahama, Th. G. .. *Geochemistry.*

Romo, L. A. and Roy, Rustom *Am. Min.*, 1957, **42**, 165.

Sadashiviah, M. S. and Ghosh, S. D. *Proc. Ind. Acad. Sci.*, 1953, **37**, 752.

Sahama, Th. G. .. *Annales Acad. Sci.*, Fennicæ, 1953, **3 A** (31).

Sjogren, Hj. .. *Bull. Geol. Inst. Upsala*, 1893, **1** (1).

Sjogren, Hj. .. *Bull. Geol. Inst. Upsala*, 1894, **2** (3).

Taylor, W. H. and West, J. .. *Proc. Roy. Soc. Lond.*, 1928, **117 A**, 517.

———— .. *Zeitschr. Krist. Bd.*, 1929, **70**, 461.

Thiele .. *Chemie der Er.*, 1940, **13**, 73.

Van Valkenburg, J. R. .. *Am. Min.*, 1955, **40**, 339.

Walker, T. L. and Parsons, A. L. *Univ. Toronto Series, Geol. Ser.*, 1927, **24**, 15.

West, W. D. .. *Trans. Nat. Inst. of Sci. India*, 1936, **1** (6), 93.

Winchell, A. N. and Winchell, H. *Elements of Optical Mineralogy*, Part II.

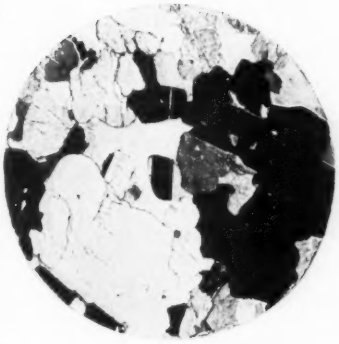

FIG. 1. Clinohumite—Symmetrical extinction. × 12.

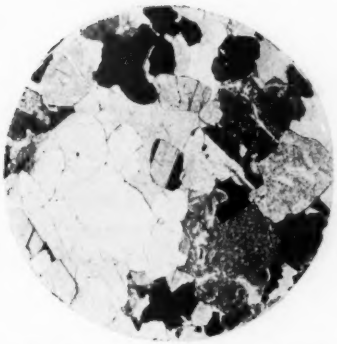

FIG. 2 Clinohumite—Symmetrical extinction. × 12.

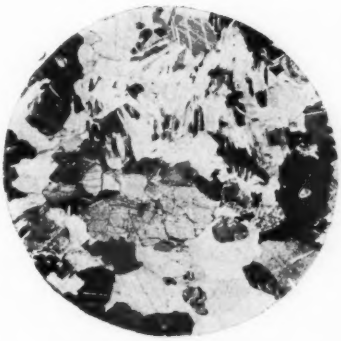

FIG. 3. Clinohumite with calcite, forsterite, tremolite and spinel. × 12.

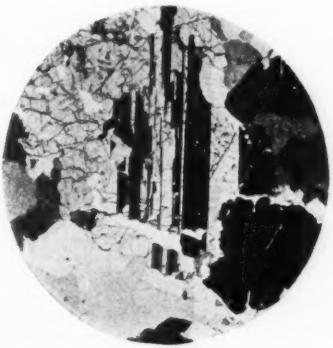

FIG. 4. Clinohumite—Polysynthetically twinned. × 8.

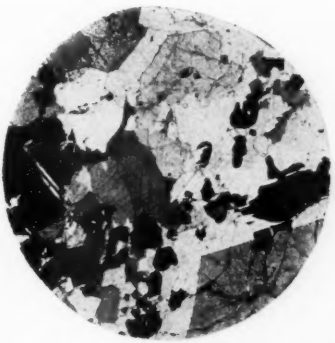

FIG. 5. Clinohumite with calcite, spinel and phlogopite. × 12.

STUDIES ON THE RELATION BETWEEN CHEMICAL CONSTITUTION AND ULTRAVIOLET ABSORPTION SPECTRA OF OPTICALLY ACTIVE AND RACEMIC COMPOUNDS

Part VII. Correlation of Absorption Maxima, $\lambda_{max.}$ and Characteristic Wavelengths, λ_{0s}, of Camphor-β-Sulphonyl-phenyl, -tolyl (*o*-, *m*- and *p*-) and Naphthyl (α- and β-)-amides

By Bawa Kartar Singh, F.A.Sc. and Shiva Mohan Verma

(Organic Chemistry Research Section, Banaras Hindu University)

Received March 19, 1958

Abstract

The ultraviolet absorption spectra of camphor-β-sulphonyl-phenyl, (*o*-, *m*- and *p*-) tolyl, (α- and β-) naphthylamides have been determined in methyl alcohol, ethyl alcohol, and chloroform. The absorption spectra of all the compounds show two absorption bands: one varying from 267 to 284 mμ, the longer absorption maximum ($\lambda_{max.}$) due to selective absorption of the keto group, and the other shorter one, ranging from 226 to 230 mμ, due to general absorption of the saturated molecules. The values of the characteristic wavelengths, λ_{0s}, obtained from Drude's one-term equation, have been compared with the absorption maxima, $\lambda_{max.}$, obtained by direct measurements. There are marked discrepancies in the values of λ_0 and $\lambda_{max.}$ An explanation of the discrepancies is given.

The nature of racemic modifications of the compounds has also been discussed.

In continuation of Part VI[1] of this series, we describe, in this communication, the ultraviolet absorption spectra of (*d* and *dl*) camphor-β-sulphonyl-phenyl, *o*-tolyl, *m*-tolyl, *p*-tolyl and naphthyl (α- and β-)-amides in methyl alcohol, ethyl alcohol and chloroform. The 'characteristic' wavelengths, λ_{0s}, calculated from Drude's rotatory dispersion *one-term* equation[2] have been compared with the absorption maxima, $\lambda_{max.}$, obtained by direct measurements.

The absorption measurements of the dextro and the racemic forms of these compounds have been studied with a view to throw further light on the nature of these racemic modifications investigated by us[2] earlier by the application of melting point-composition diagram of Roozeboom,

EXPERIMENTAL

The compounds mentioned above were prepared and purified according to methods described previously.[2] The absorption measurements were carried out in spectroscopically pure solvents with Beckman DU Spectrophotometer. The molecular extinction coefficients, ϵ, were calculated from optical density at different wavelengths, but only their peak values ($\epsilon_{max.}$) corresponding to the absorption maxima, $\lambda_{max.}$, are given in Table I. The absorption spectra curves (Figs. 1–6) were prepared by plotting the molecular extinction coefficients (ϵ) against the corresponding wavelengths (λ).

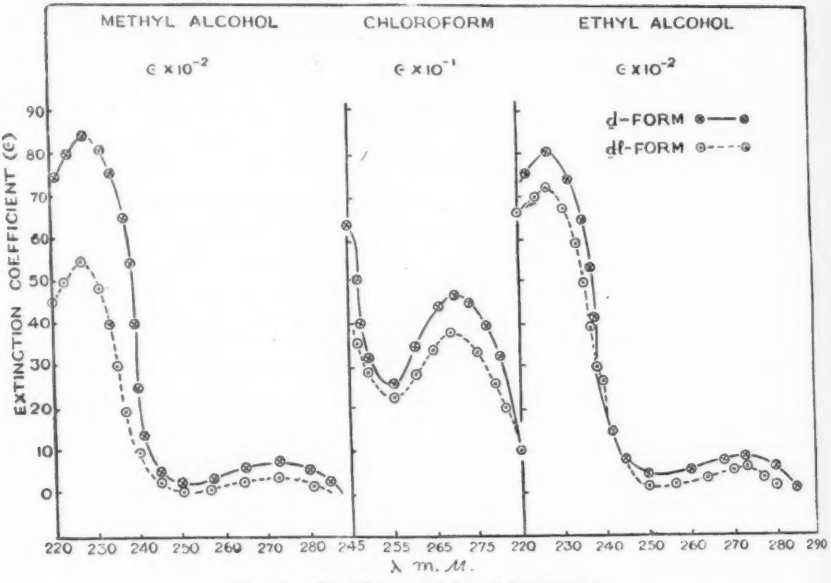

FIG. 1. Camphor-β-sulphonylphenylamides.

The rotatory dispersion of *d*-camphor-β-sulphonyl-α-naphthylamide, which was not given in chloroform in the earlier paper,[2] has been determined and recorded in Table VI.

DISCUSSION

The most frequent representation of rotatory dispersion is given by Drude's equation,

$$[\alpha] = \sum \frac{K}{\lambda^2 - \lambda_0^2},$$

TABLE I

TABLE I

Compound	Solvent	*d*-isomer		*dl*-isomer		λ_0 in mμ*	$\lambda_0-\lambda_{max.}$
		$\lambda_{max.}$ mμ	$\epsilon_{max.}$	$\lambda_{max.}$ mμ	$\epsilon_{max.}$		
Camphor-β-sulphonyl† phenylamide ..	Methyl alcohol	273 228	724·5 8442·5	273 227	260·95 5372·5	296·6	+23·6
Camphor-β-sulphonyl† phenylamide ..	Ethyl alcohol	273 227	808·9 8025·0	273 227	540·5 7042·0	295·0	+22·0
Camphor-β-sulphonyl† phenylamide ..	Chloroform	270 ..	460·5 ..	271 ..	375·0 ..	255·0	−16·0
Camphor-β-sulphonyl-*o*-tolylamide	Methyl alcohol	267 226	680·5 6442·0	267 226	638·8 7608·0	279·3	+12·3
Camphor-β-sulphonyl-*o*-tolylamide ..	Ethyl alcohol	267 226	609·9 7254·6	267 226	555·3 7062·0	249·0	−18·0
Camphor-β-sulphonyl-*o*-tolylamide ..	Chloroform	267 ..	890·0 ..	267 ..	492·0 ..	204·9	−62·1
Camphor-β-sulphonyl-*m*-tolylamide ..	Methyl alcohol	275 230	658·0 12040·0	275 230	1034·0 9469·0	279·3	+ 4·3
Camphor-β-sulphonyl-*m*-tolylamide ..	Ethyl alcohol	275 230	914·15 14686·0	275 230	590·6 7543·5	286·4	+11·4
Camphor-β-sulphonyl-*m*-tolylamide ..	Chloroform	273 ..	882·8 ..	273 ..	327·4 ..	235·9	−37·1

TABLE I—*Contd.*

Compound	Solvent	*d*-isomer		*dl*-isomer		λ_0 in mμ*	$\lambda_0-\lambda_{max.}$
		$\lambda_{max.}$ mμ	$\epsilon_{max.}$	$\lambda_{max.}$ mμ	$\epsilon_{max.}$		
Camphor-β-sulphonyl-*p*-tolylamide ..	Methyl alcohol	278 230	706·2 8667·0	278 230	738·3 9148·5	289·8	+11·8
Camphor-β-sulphonyl-*p*-tolylamide ..	Ethyl alcohol	278 230	741·5 7961·0	278 230	619·5 8506·5	277·5	− ·5
Camphor-β-sulphonyl-*p*-tolylamide ..	Chloro-form	276 ..	497·5 ..	276 ..	677·3 ..	242·9	−33·1
Camphor-β-sulphonyl-α-naphthylamide ..	Methyl alcohol	284 230	6569·0 9925·0	284 228	5348 9353	321·0	+37·0
Camphor-β-sulphonyl-α-naphthylamide ..	Ethyl alcohol	285 230	6590·0 9710·4	285 230	5536 9462·0	288·0	+ 3·0
Camphor-β-sulphonyl-α-naphthylamide ..	Chloro-form	287 ..	4213 ..	287 ..	6051 ..	233·4	−53·6
Camphor-β-sulphonyl-β-naphthylamide ..	Methyl alcohol	278 235	4891·0 10353·0	278 235	4177 9460	300·2	+22·2
Camphor-β-sulphonyl-β-naphthylamide ..	Ethyl alcohol	278 235	4641·0 9817·5	278 235	4712·4 9817·5	282·3	+ 4·3
Camphor-β-sulphonyl-β-naphthylamide ..	Chloro-form	280 ..	3463 ..	280 ..	5783 ..	252·8	−27·2

* λ_{∞} obtained from Drude's one-term equation.[2]

† *d*-Camphor-β-sulphonyl-*m*-tolylamide was taken in 0·004 per cent. concentration, whereas 0·01 per cent. solutions of all the other compounds were used.

EXTINCTION COEFFICIENT (ε)

EXTINCTION COEFFICIENT (ε)

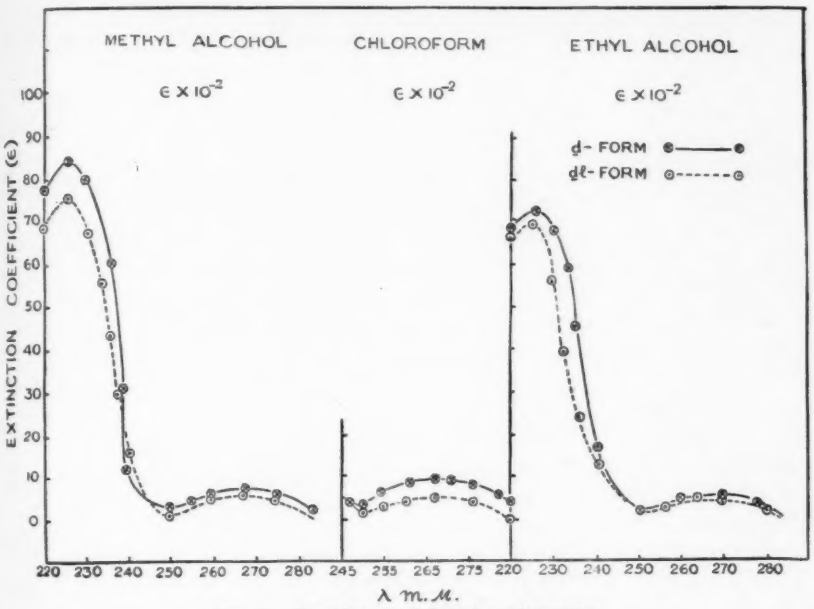

FIG. 2. Camphor-β-sulphonyl-*o*-tolylamides.

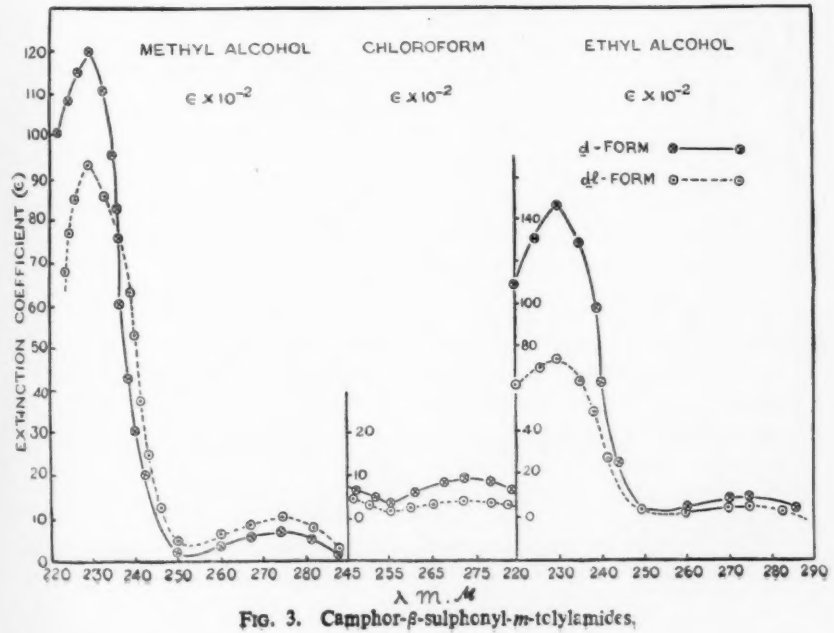

FIG. 3. Camphor-β-sulphonyl-*m*-tolylamides.

* λ_{max} obtained from Drude's one-term equation.[2]
† *d*-Camphor-β-sulphonyl-*m*-tolylamide was taken in 0·004 per cent. concentration, whereas 0·01 per cent. solutions of all the other compounds were used.

In this equation the summation contains several partial rotation terms, such as,

$$\frac{K'}{\lambda^2 - \lambda_0'^2}, \quad \frac{K''}{\lambda^2 - \lambda_0''^2}, \quad \frac{K'''}{\lambda^2 - \lambda_0'''^2} \cdots$$

where K′, K″, K‴, ... , etc., represent the rotation constants and λ_0', λ_0'', λ_0''', etc., the 'characteristic' wavelengths governing the rotation. According to theoretical considerations, the 'characteristic' wavelengths, λ_{0s}, are those at which the molecule absorbs radiation strongly and these should correspond to the frequencies of the equivalent classical electronic oscillators in the molecules. In the case of most optically active organic compounds, it is found that the one-term Drude equation,

$$[\alpha] = \frac{K}{\lambda^2 - \lambda_0^2},$$

is usually sufficient to fit the observed values of rotations. The value of λ_0 in this equation should be equal to the absorption band in the ultraviolet or visible region of the spectrum.

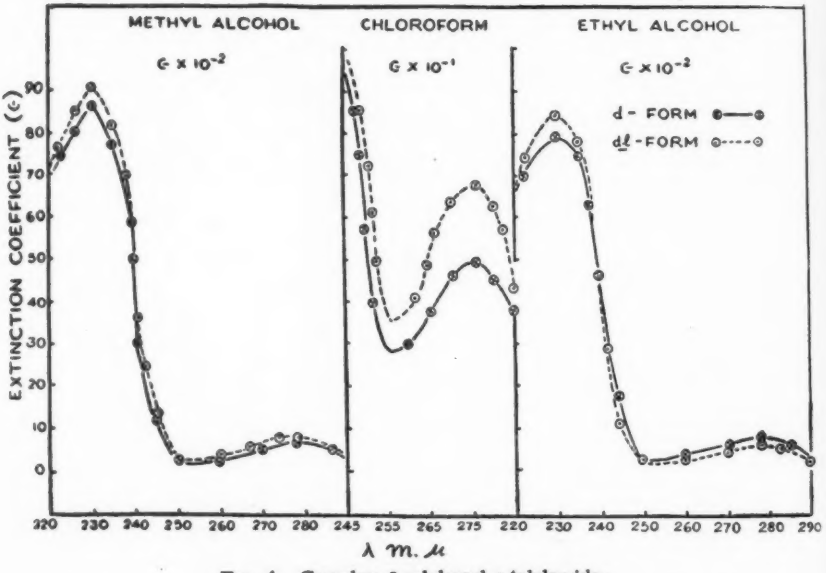

FIG. 4. Camphor-β-sulphonyl-*p*-tolylamides.

As stated in the previous communications,[3-5] generally the rotatory dispersion is expressed by one- or two-term Drude's formula, whereas the sum-

mation includes several terms of which the one or two terms may be more important than the succeeding ones, which either are too small or may nearly cancel each other and are, therefore, neglected. It is, thus, clear that this mode of representation by one- or two-term formula is far from reality. The terms found necessary in one- or two-term equation of Drude, within the limits of experimental error, thus, approximately represent the main contribution to the optical activity. In this paper we have shown that the one-term (*simple*), as well as the two-term (*complex*) equation of Drude, both equally well represent the observed rotatory dispersion of the compounds

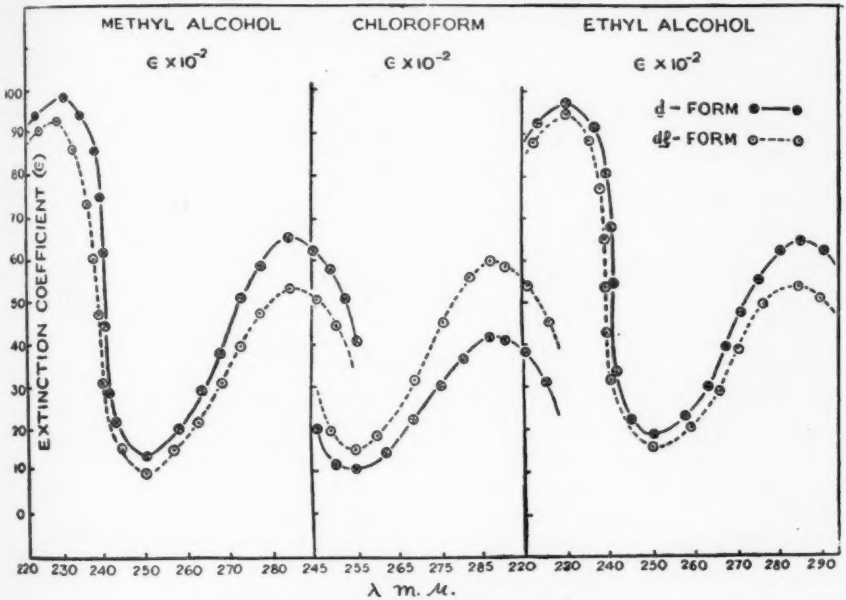

FIG. 5. Camphor-β-sulphonyl-α-naphthylamides.

within the limits of experimental accuracy (Tables II–VI). The rotatory dispersion of the compounds had already been reported '*simple*' as the observed values were in good agreement with those calculated from the *one-term* equation (Tables II–VI) but the characteristic wavelengths derived from the dispersion constants of these equations do not agree with the absorption maxima, $\lambda_{max.}$, obtained by our present measurements (Table I). In the column of differences, $\lambda_0 - \lambda_{max.}$ (Table I), these values range from $-\cdot 5$ to $-62\cdot 1$ mμ, which are, therefore, considerable in several cases. Working in the reverse way, by substituting both the absorption maxima ($\lambda_{1\ max.}$ and

$\lambda_{2\ max.}$) for the characteristic wavelengths (λ_{0s}), governing the rotation, in the two-term (complex) Drude formula for rotatory dispersion, namely,

$$[\alpha] = \frac{K_1}{\lambda^2 - \lambda_{1\ max.}^2} + \frac{K_2}{\lambda^2 - \lambda_{2\ max.}^2},$$

we find that the values of the rotatory powers calculated from these two-term (complex) formulæ like those from one-term (simple) formulæ already reported agree equally well with the observed values of rotatory power (Tables II–VI). The 'characteristic' wavelengths (λ_{0s}) derived from one-term formula, being different from the absorption maxima ($\lambda_{max.}$) obtained experimentally, are thus hypothetical, which explains the discrepancies between them.

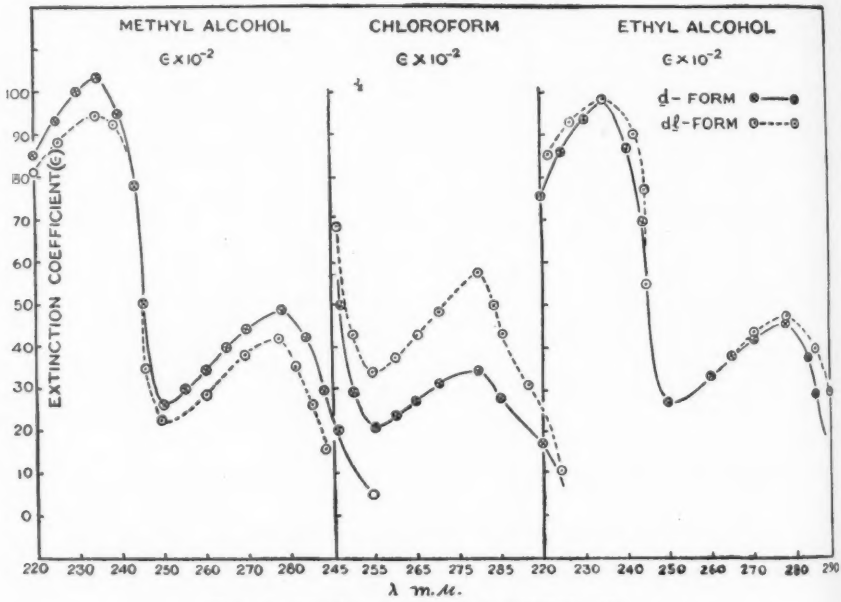

FIG. 6. Camphor-β-sulphonyl-β-naphthylamides.

ABSORPTION SPECTRA CURVES OF CAMPHOR-β-SULPHONYL-PHENYL, *o*-TOLYL, *m*-TOLYL, *p*-TOLYL, α-NAPHTHYL AND β-NAPHTHYLAMIDES

The ultraviolet absorption spectra curves of camphor-β-sulphonyl-phenyl (Fig. 1), *o*-tolyl (Fig. 2), *m*-tolyl (Fig. 3), *p*-tolyl (Fig. 4), α-naphthyl (Fig. 5) and β-naphthyl (Fig. 6) amides (*d* and *dl*) in methyl alcohol, ethyl alcohol and chloroform (chloroform not transparent below 245 mμ) are

TABLE II

Rotatory dispersion of d*-camphor-β-sulphonyl phenylamide at 35° C.*

Solvent	Methyl alcohol					Chloroform				
	Observed	Calculated				Observed	Calculated			
Equation	$[\alpha]$	$[\alpha]=\frac{7\cdot292}{\lambda^2-0\cdot088}$		$[\alpha]=\frac{17\cdot22}{\lambda^2-0\cdot0745}-\frac{10\cdot412}{\lambda^2-0\cdot052}$		$[\alpha]$	$[\alpha]=\frac{20\cdot4}{\lambda^2-0\cdot065}$		$[\alpha]=\frac{9\cdot866}{\lambda^2-0\cdot0745}+\frac{10\cdot637}{\lambda^2-0\cdot052}$	
Lines (Å)	o	c	$o-c$	c	$o-c$	o	c	$o-c$	c	$o-c$
6708 ..	19·5	20·14	− ·64	19·69	− ·19	53·0	52·98	+ ·02	52·99	+ ·01
6438 ..	22·0	22·32	− ·32	21·94	+ ·06	58·0	58·37	− ·37	58·35	− ·35
6104 ..	25·5	25·63	− ·13	25·5	± ·0	67·5	66·34	+1·16	66·28	+1·22
5893 ..	28·0	28·13	− ·13	27·87	+ ·13	73·0	72·30	+ ·70	72·2	+ ·8
5780 ..	29·5	29·64	− ·14	29·4	+ ·10	76·5	75·82	+ ·68	75·7	+ ·8
5468 ..	34·5	34·55	− ·05	34·55	− ·05	87·0	87·18	− ·18	87·0	± ·0
5461 ..	34·5	34·69	− ·19	34·68	− ·18	87·0	87·48	− ·48	87·3	− ·3
5209 ..	40·5	39·77	+ ·73	40·02	+ ·48	100·0	98·88	+1·12	98·63	+1·37
5086 ..	43·0	42·75	+ ·25	43·10	− ·10	105·0	105·4	−0·4	105·07	− ·07
4800 ..	51·0	51·21	− ·21	52·09	−1·09	120·0	123·3	−3·3	122·9	−2·9
4678 ..	57·5	55·76	+1·74	57·01	+ ·49	131·5	132·5	−1·0	132·14	− ·64
4603 ..	60·0	58·89	+1·11	60·26	− ·26	138·0	139·0	−1·0	138·42	− ·42
4358 ..	73·0	71·48	+1·52	73·64	− ·64	162·5	163·2	−0·7	162·48	+ ·02

TABLE III

Rotatory dispersion of d*-camphor-β-sulphonyl-*o*-tolylamide at 35° C.*

Solvent	Methyl alcohol					Chloroform				
	Observed	Calculated				Observed	Calculated			
Equation	$[\alpha]$	$[\alpha]=\frac{8\cdot835}{\lambda^2-0\cdot078}$		$[\alpha]=\frac{15\cdot42}{\lambda^2-0\cdot0713}-\frac{6\cdot886}{\lambda^2-0\cdot0511}$		$[\alpha]$	$[\alpha]=\frac{14\cdot506}{\lambda^2-0\cdot506}$		$[\alpha]=\frac{5\cdot651}{\lambda^2-0\cdot0713}+\frac{20\cdot155}{\lambda^2-0\cdot0511}$	
Lines (A)	o	c	$o-c$	c	$o-c$	o	c	$o-c$	c	$o-c$
6708 ..	23·5	23·75	− ·25	23·45	+·05	36·0	35·55	+ ·45	35·60	+ ·4
6438 ..	26·0	26·26	− ·26	25·98	+·02	39·0	38·94	+ ·06	39·00	± ·0
6104 ..	30·0	30·00	± ·0	29·77	+·23	45·0	43·89	+1·11	43·95	+1·05
5893 ..	32·5	32·82	− ·32	32·64	−·14	47·5	47·52	− ·02	47·98	− ·48
5780 ..	34·5	34·51	− ·01	34·35	+·15	50·0	49·62	+ ·38	49·73	+ ·27
5468 ..	40·0	39·97	+ ·03	40·01	−·01	56·5	56·44	+ ·06	56·5	± ·0
5461 ..	40·0	40·13	− ·13	40·09	−·09	57·0	56·62	+ ·38	56·66	+ ·34
5209 ..	45·5	45·69	− ·19	45·83	−·33	63·0	63·25	− ·25	63·28	− ·28
5086 ..	49·0	48·93	+ ·07	49·15	−·15	65·5	66·95	−1·45	66·96	−1·46
4800 ..	58·0	57·98	+ ·02	58·52	−·52	77·0	76·89	+ ·11	76·89	+0·11
4678 ..	62·5	62·76	− ·26	63·48	+·02	83·5	82·04	+1·46	81·87	+1·73
4603 ..	66·5	66·03	+ ·47	66·90	−·40	86·5	85·41	+1·09	85·2	+1·3
4358 ..	80·5	78·89	+1·61	80·34	+·16	97·5	98·06	− ·56	97·5	+0

TABLE IV

Rotatory dispersion of d-*camphor-β-sulphonyl* m-*tolylamide at* 35° *C.*

Solvent	Methyl alcohol					Chloroform				
	Observed	Calculated				Observed	Calculated			
Equation	$[\alpha]$	$[\alpha] = \frac{8\cdot028}{\lambda^2-0\cdot078}$		$[\alpha] = \frac{8\cdot654}{\lambda^2-0\cdot0756} - \frac{0\cdot0637}{\lambda^2-0\cdot0529}$		$[\alpha]$	$[\alpha] = \frac{19\cdot909}{\lambda^2-0\cdot0557}$		$[\alpha] = \frac{1\cdot275}{\lambda^2-0\cdot0756} + \frac{18\cdot856}{\lambda^2-0\cdot0529}$	
Lines (Å)	*o*	*c*	*o*−*c*	*c*	*o*−*c*	*o*	*c*	*o*−*c*	*c*	*o*−*c*
6708 ..	21·5	21·58	− ·08	21·5	± ·0	51·0	50·51	+ ·49	50·89	+ ·11
6438 ..	23·5	23·86	− ·36	23·77	− ·27	55·5	55·49	+ ·01	55·91	− ·41
6104 ..	27·0	27·27	− ·27	27·15	− ·15	63·5	62·85	+ ·65	63·28	+ ·22
5893 ..	29·5	29·82	− ·32	29·70	− ·20	68·0	68·31	− ·31	68·76	− ·76
5780 ..	31·5	31·36	+ ·14	31·23	+ ·27	72·0	71·55	+ ·45	72·0	± ·0
5468 ..	36·5	36·33	+ ·17	36·14	+ ·36	82·0	81·85	+ ·15	82·33	− ·33
5461 ..	36·5	36·46	+ ·04	36·30	+ ·20	82·0	82·12	− ·12	82·59	− ·59
5209 ..	41·5	41·53	− ·03	41·31	+ ·19	92·0	92·37	− ·37	92·85	− ·85
5086 ..	44·0	44·45	− ·45	44·19	− ·19	98·5	98·13	+ ·37	98·62	− ·12
4800 ..	51·5	52·09	− ·59	52·32	− ·82	114·5	114·0	− ·5	114·46	+ ·04
4678 ..	55·5	57·03	−1·53	56·59	−1·09	122·5	122·1	+ ·4	122·56	− ·06
4603 ..	60·0	59·99	+ ·01	59·53	+ ·47	130·0	127·6	+2·4	128·02	+1·98
4358 ..	71·0	71·68	− ·68	71·0	± ·0	149·0	148·3	+ ·7	148·68	+ ·32

TABLE V

Rotatory dispersion of d-*camphor-β-sulphonyl*-p-*tolylamide at 35° C.*

Solvent	Methyl alcohol					Chloroform				
	Observed	Calculated				Observed	Calculated			
Equation	$[\alpha]$	$[\alpha]=\frac{7\cdot9296}{\lambda^2-0\cdot0841}$		$[\alpha]=\frac{9\cdot225}{\lambda^2-0\cdot0773}-\frac{1\cdot1956}{\lambda^2-0\cdot0529}$		$[\alpha]$	$[\alpha]=\frac{20\cdot137}{\lambda^2-0\cdot059}$		$[\alpha]=\frac{4\cdot327}{\lambda^2-0\cdot0773}+\frac{15\cdot846}{\lambda^2-0\cdot0529}$	
Lines (Å)	o	c	$o-c$	c	$o-c$	o	c	c	c	$o-c$
6708 ..	22·0	21·67	+ ·33	21·74	+ ·26	51·5	51·48	+ ·02	51·5	± ·0
6438 ..	24·0	24·0	± ·0	24·04	− ·04	56·5	56·63	− ·13	56·65	− ·15
6104 ..	27·5	27·49	+ ·01	27·50	± ·0	64·5	64·22	+ ·28	64·24	+ ·26
5893 ..	30·0	30·13	− ·13	30·11	− ·11	70·0	69·85	+ ·15	69·85	+ ·15
5780 ..	32·0	31·76	+ ·24	31·67	+ ·33	74·0	73·21	+ ·79	73·23	+ ·77
5468 ..	37·0	36·90	+ ·10	36·76	+ ·24	84·0	83·89	+ ·11	83·89	+ ·11
5461 ..	37·0	37·03	− ·03	36·89	+ ·11	84·0	84·26	− ·26	84·17	− ·17
5209 ..	42·0	42·35	− ·35	42·07	− ·07	96·0	94·84	+1·16	94·80	+1·2
5086 ..	45·0	45·44	− ·44	45·06	− ·06	101·0	100·0	+1·0	100·89	+ ·11
4800 ..	54·0	54·19	− ·19	53·51	+ ·49	117·5	117·4	+ ·1	117·55	− ·05
4678 ..	59·0	58·86	+ ·14	57·98	+1·02	128·5	126·0	+2·5	126·08	+2·42
4603 ..	61·5	62·90	−1·4	61·06	+ ·44	133·0	131·8	+1·2	131·89	+1·11
4358 ..	73·0	74·87	−1·87	73·13	− ·13	154·0	153·3	+ ·7	154·0	± ·0

practically identical. The absorption curves of the dextro and the racemic forms of these compounds in different solvents (Figs. 1–6) show two maxima, one a weak band, $\lambda_{max.}$ varying from 267–84 mμ which is due to the selective absorption of the free keto group present in the compounds and the other, an intense band, $\lambda_{max.}$ ranging from 226–30 mμ—due to general absorption of the saturated molecules. Camphor-β-sulphonyl phenylamide shows selective absorption at the longer wavelength ($\lambda_{max.}$ 273 mμ, $\epsilon_{max.}$ 460·5–808·9 in different solvents, Table I) and the substitution of a methyl group in the *ortho* position of the phenyl nucleus shifts the absorption maximum towards the shorter wavelength side ($\lambda_{max.}$ 267 mμ, $\epsilon_{max.}$ 609·9–680), whereas this group in the *meta* position ($\lambda_{max.}$ 275 mμ, $\epsilon_{max.}$ 658–914·15) and in the *para* position ($\lambda_{max.}$ 278 mμ, $\epsilon_{max.}$ 497·5–741·5) shifts them towards the longer wavelength side (bathochromic effect).

TABLE VI

Rotatory dispersion of d-*camphor-*β*-sulphonyl-*α*-naphthylamide at* 35° *C.*

Solvent		Chloroform (1 per cent. solution)			
Equation	Observed [α]	Calculated $[\alpha] = \frac{14{\cdot}63}{\lambda^2-0{\cdot}0545}$		$[\alpha] = \frac{1{\cdot}55}{\lambda^2-0{\cdot}0807} + \frac{13{\cdot}0}{\lambda^2-0{\cdot}0529}$	
Lines (Å)	*o*	*c*	*o*—*c*	*c*	*o*—*c*
6708	37·0	36·99	+ ·01	36·93	+ ·07
6438	40·0	40·63	— ·63	40·59	— ·59
6104	46·0	46·0	± 0	45·99	+ ·01
5893	50·0	49·98	+ ·02	50·01	— ·01
5780	52·0	52·28	— ·28	52·36	— ·36
5468	60·0	59·83	+ ·17	59·92	+ ·08
5461	60·0	60·03	— ·03	60·11	— ·11
5209	67·0	67·48	— ·48	67·65	— ·65
5086	71·0	71·68	— ·68	71·90	— ·90
4800	82·0	83·17	—1·17	83·58	—1·58
4678	90·0	89·04	+ ·96	89·58	+ ·42
4603	93·0	93·0	± ·0	93·63	— ·63
4358	109·0	107·97	+1·03	109·0	± 0

The bathochromic shift of the ketonic band is also observed when the phenyl group of camphor-β-sulphonyl phenylamide (273 mμ) is replaced by napthyl groups (α-, $\lambda_{max.}$ 284 mμ, $\epsilon_{max.}$ 4213–6590 and β-, $\lambda_{max.}$ 278 mμ, $\epsilon_{max.}$ 3463–4891). The absorption maxima of the naphthyl ($\lambda_{max.}$ = 275 mμ) and

the keto ($\lambda_{max.} = 278$ mμ) groups are nearly equal but the absorptive power ($\epsilon_{max.}$) of the naphthyl group is much greater than that of the keto. The weaker absorption band of the keto group is thus submerged in the more intense band of the naphthyl group (Figs. 5 & 6 and Table I).

NATURE OF THE RACEMIC FORMS

The racemic forms of the optically active compounds were found to be racemates (*dl*) in the solid state[2] by the melting point-composition method of Roozeboom. The ultraviolet absorption spectra of the racemic forms have been now found to be nearly identical with those of the corresponding dextro forms (Figs. 1–6): the slight differences being in the values of molecular extinction coefficients, ϵ, in the two cases, whereas the values of absorption maxima ($\lambda_{max.}$) are identical (Table I). From the nearly identical absorption spectra curves for the dextro and racemic forms, it may be concluded that the racemic forms have almost completely dissociated in very dilute solutions into the optically active and opposite forms.

ACKNOWLEDGEMENT

We thank the Banaras Hindu University for providing research facilities, and the Government of India, Ministry of Education, for the award of a Senior Research Scholarship to one of us (S. M. Verma).

REFERENCES

1. Singh, B. K. and Verma, S. M. .. *J. Sci. and Ind. Res.*, 1958, **17 B**, 184.
2. ———— .. *Proc. Ind. Acad. Sci.*, 1956, **43**, 21.
3. ——— and Kapur, N. S. .. *J. Sci. and Ind. Res.*, 1958, **17 B**, in the Press.
4. ——— and Saxena, B. S. .. *J. Ind. Chem. Soc.*, 1958, **35**, 227.
5. ——— and Sarma, S. R. G. .. *Ibid.*, 1958, **35**, in the Press.

POLAROGRAPHIC REDUCTION OF PYRUVIC ACID

By K. S. G. Doss, F.A.Sc. and (Mrs.) Sarada Menon

(Central Electro-Chemical Research Institute, Alagappa College P.O., Karaikudi)

Received April 28, 1958

Abstract

The application of Delahay's theory of kinetic polarographic currents as applied to the reduction of pyruvic acid has been examined. It is shown that the agreement between Delahay's theory and the available data is more satisfactory, if one assumes that the current is controlled by the rate of the reaction between pyruvate ion and water molecule forming pyruvic acid and hydroxyl ion, than when one assumes the mechanism suggested by the earlier workers involving the rate of reaction between pyruvate ion and hydrogen-ion, both from the point of view of the magnitude of the diffusion current as well as its pH dependence. The results give an indication of the latter reaction being sluggish due to the activation energy requirements.

The reduction of pyruvic acid at the dropping mercury electrode has been studied by a number of workers.[1] A systematic study in buffer solution was made by Muller and Baumberger[2] who showed that at pH values smaller than 4·1 only one wave occurs. At higher pH values, upto a pH of 8, two waves are observed. The first wave, which occurs at all the pH values, corresponds to the reduction of the free acid as shown by Brdicka.[3] Delahay[4] worked out the formulation for the kinetic polarographic currents and applied the theory to the data obtained on the reduction of pyruvic acid.[5] The object of the present paper is to examine the possible mechanisms for the reduction of undissociated pyruvic acid in relation to the general theory of Delahay and the available experimental data.

An examination of the values of diffusion currents for the first wave for the reduction of pyruvic acid at different pH values shows that at the higher pH values, the observed diffusion current is much higher than the value got from the Ilkovic equation on the basis of the concentration of the undissociated acid. For example, at a pH of 6·87, the concentration of the free acid would be 7×10^{-8} mole per litre and the corresponding calculated diffusion current would be about 3×10^{-4} microamp.[5] The observed value, however, is 0·42 microamp., which is greater than the theoretical

value by a factor of about 100,000. It is obvious, therefore, that this is a case wherein the polarographic current is determined not only by the diffusion of existing free acid molecules but also by the diffusion of the undissociated acid molecules formed from the anions.

The following are the two mechanisms which can give rise to the undissociated molecule:

(i) $A^- + H_3O^+ \rightleftarrows HA + H_2O$

(ii) $A^- + H_2O \rightleftarrows HA + OH^-$.

Delahay has applied his theory for the mechanism (i), which will be discussed first. Whereas the resulting equation for the diffusion current is generally in agreement with the experimental data, he has pointed out[4] that the value for k_r calculated on the basis of mechanism (i) from the observed diffusion current comes out to be $2{\cdot}12\times10^{11}$ (moles per c.c.)$^{-1}$ sec.$^{-1}$ The application of the Onsager's theory of combination of ions[5] would, on the other hand, lead to a value of $5{\cdot}1\times10^{13}$ sec.$^{-1}$ (moles per c.c.).$^{-1}$ Thus the polarographic value of k_r on the basis of mechanism (i) comes out to be more than 200 times smaller as compared with the value based on Onsager's theory. Furthermore, if one calculates the polarographic value of k_r from Delahay's data corresponding to a pH of 6·11, one gets a value about 2,000 times smaller than that got on the basis of Onsager's theory.

Let us now examine the pH dependence of the diffusion current in relation to the mechanism (i). The equation for polarographic current comes out to be

$$i_{av} = 0{\cdot}6 \times 1{\cdot}255 \times 10^6 m^{\frac{2}{3}}\tau^{\frac{1}{3}}C^0_{H_3O^+}\, C_{A^-}\, D^{\frac{1}{2}}_{HA}\left[\frac{k_r}{K}^{\frac{1}{2}}\right], \qquad (1)$$

where K is the dissociation constant of pyruvic acid in moles per litre, k_r the Onsager's Coefficient for recombination of pyruvate and hydrogen-ion in (moles per litre)$^{-1}$ sec.$^{-1}$, $C^0_{H_3O^+}$ and C_{A^-} are the bulk concentrations of hydrogen-ion and pyruvate ion in moles per litre, m and τ are the capillary constants in mg. per sec., and sec. respectively, and D_{HA} is the diffusion coefficient of pyruvic acid in cm.^{2} sec.$^{-1}$

It is clear therefore that the diffusion current is proportional to $C_{H_3O^+}\times C_{A^-}$. Since the pK of pyruvic acid is 2·55, the concentration of undissociated pyruvic acid would be negligible at pH values greater than 4·55. Thus for pH values greater than 4·55, one can replace C_{A^-} in equation (1), by the

total concentration of pyruvic acid. At constant total concentration of pyruvic acid, one gets the relation:

$$i_{av} \propto C_{H_3O^+}$$

or

$$\log i_{av} + pH = K_i. \tag{2}$$

The values of i_{av} corresponding to the various values of pH are taken from Delahay's paper.[5] Table I, column 3 contains the values of the constant as per relation in equation (2). An examination of the values shows that the constant varies from 4·96 to 6·49.

TABLE I

i_{av} (microamps.)	pH	K_i	K_{ii}
5·78	4·2	4·96	2·86
5·21	5·2	5·92	3·32
3·35	5·89	6·42	3·48
2·45	5·95	6·34	3·37
1·04	6·11	6·13	3·08
0·79	6·32	6·22	3·06
0·65	6·56	6·37	3·09
0·42	6·87	6·49	3·06

We shall now proceed to examine mechanism (ii). Applying Delahay's theory, we get,

$$\left(\frac{\partial C_{HA}}{\partial t}\right)_{x,t} = D_{HA} \frac{\partial^2 C_{HA}}{\partial x^2} + k_r C_{OH^-} \{C^0_{HA} - C_{HA}\} \tag{3}$$

where C_{HA} is the concentration of pyruvic acid near the interface at a distance x and time t, k_r kinetic theory constant for the reaction between HA and OH^- and C^0_{HA} is the bulk concentration of pyruvic acid. It is assumed that C_{OH^-} is the same at the interface and the bulk. Putting the appropriate

boundary conditions, applying the Laplace Transformation and integrating we get,

$$C_{HA} = C^0_{HA} \left\{ 1 - \tfrac{1}{2} \exp. \left[-x \left(\frac{k_\tau C_{OH^-}}{D_{HA}} \right)^{\frac{1}{2}} \right] \right.$$
$$\times \, erfc \left[\frac{x}{2 (D_{HA} t)^{\frac{1}{2}}} - (k_\tau C_{OH^-} t)^{\frac{1}{2}} \right]$$
$$- \tfrac{1}{2} \exp \left[x \left(\frac{k_\tau C_{OH^-}}{D_{HA}} \right)^{\frac{1}{2}} \right] erfc \left[\frac{x}{2 (D_{HA} t)^{\frac{1}{2}}} \right.$$
$$\left. \left. + (k_\tau C_{OH^-} t)^{\frac{1}{2}} \right] \right\}. \qquad (4)$$

From equation (4), one can calculate $D_{HA} (\partial C_{HA}/\partial x)_{x=0}$ which gives the flux of HA at the electrode. Taking into account the area of the electrode, the number of electrons involved in the electrode reaction and the constants of the capillary, and applying correction for spherical diffusion, we get, for the average polarographic current (for high values of $k_\tau C_{OH^-}$),

$$i_{av} = 1 \cdot 255 \times \frac{3}{5} \times 10^6 n m^{\frac{2}{3}} \tau^{\frac{1}{3}} D^{\frac{1}{2}}_{HA} C^0_{HA} C^{\frac{1}{2}}_{OH^-} k_\tau^{\frac{1}{2}}. \qquad (5)$$

Putting

$$C_{HA} = \frac{C_{H_3O^+} C_{A^-}}{K} \quad \text{and} \quad C^{\frac{1}{2}}_{OH^-} = \left(\frac{K_w}{C_{H_3O^+}} \right)^{\frac{1}{2}}$$

we get

$$i_{av} = \frac{3}{5} \times 1 \cdot 255 \times 10^6 r m^{\frac{2}{3}} \tau^{\frac{2}{3}} D^{\frac{1}{2}}_{HA} \frac{K_w^{\frac{1}{2}}}{K} k_\tau^{\frac{1}{2}} C^{\frac{1}{2}}_{H_3O^+} C_{A^-}. \qquad (6)$$

Applying equation (6) for the data of Delahay and putting

$$m = 1 \cdot 53 \quad \tau = 3 \cdot 85 \quad D_{HA} = 0 \cdot 44 \times 10^{-5}, \quad n = 2$$
$$K_{w(30^\circ C.)} = 1 \cdot 3 \times 10^{-14}, \quad K = 2 \cdot 8 \times 10^{-3}, \quad C_{H_3O^+} = 1 \cdot 35 \times 10^{-7} \quad (pH = 6 \cdot 87)$$
$$C_{A^-} = 1 \cdot 5 \times 10^{-3} \text{ (moles/litre)}, \quad i_{av} = 0 \cdot 42$$

we get

$$k_\tau = 3 \cdot 2 \times 10^{12} \text{ (moles/litre)}^{-1} \text{ sec.}^{-1}$$
$$= 3 \cdot 2 \times 10^{15} \text{ (moles/cm.}^3\text{)}^{-1} \text{ sec.}^{-1}$$

In the absence of any activation step, this kinetic theory constant k_r may be expected to be of the same order as the Onsager coefficient for recombination of ions (5×10^{13}). The observed value is therefore no doubt on the high side. But, the agreement is more satisfactory than with mechanism (i).

We shall now proceed to consider the pH dependence of the diffusion current on the basis of mechanism (ii). From equation (6), it is clear that,

$$i_d \propto C^{\frac{1}{2}}_{H_3O^+} C_{A^-}.$$

At high values of pH, one can replace C_{A^-} by the total concentration of pyruvic acid as already pointed out. Thus we get for any particular concentration of pyruvic acid,

$$i_d \propto C^{\frac{1}{2}}_{H_3O^+}$$

or

$$\log\ i_d + \tfrac{1}{2}\mathrm{pH} = K_{ii}. \qquad (7)$$

The values of K_{ii} of equation (7) as worked out from Delahay's data are given in Table I, column 4. One can see from these values that the constants show less variation than what was obtained for mechanism (i) (*cf.* column 3).

It is clear from the above discussion that mechanism (ii) is in more satisfactory agreement than mechanism (i) with the experimental data; this is particularly striking in the region of higher pH.*

It is of interest to examine the possible factors which may cause the failure of mechanism (i). The only important factor appears to be that the equilibrium represented by the mechanism (i) is highly sluggish and therefore becomes inoperative. In fact it would be sufficient if the sluggishness corresponds to one out of hundred thousand collisions being effective in the recombination of pyruvate and hydrogen-ion. It is of interest to examine this by suitable relaxation methods. The reaction between OH^- and HA on the other hand appears to be a fast reaction, every collision being effective in bringing about the reaction.

It is of interest to consider the factors which can increase the value of k_r above that given by the Onsager theory. A similar result was observed

* The deviation at lower pH is perhaps due to the change in the composition of the buffer. At pH values lower than 6, the phthalate buffers have been used whereas phosphate buffers are used at higher pH.

by one of us while working out the theory of auto-inhibition of fluorescence[6]; a close examination of the case indicated polymerisation as the cause. Similarly, the present higher value may be connected with a tendency on the part of the undissociated pyruvic acid and the hydroxyl ion to form a complex. This inference however is purely tentative, since effect of other factors such as the activity coefficient, adsorption at the interface, etc., would have to be taken into account, before a final conclusion is reached.

REFERENCES

1. Kolthoff, M. and Lingane, J. J. — *Polarography*, Interscience Publishers Inc., New York, 2nd edition, 1952, p. 729, Ref. 41.
2. Muller, O. H. and Baumberger, J. P. — *J. Am. Chem. Soc.*, 1939, **61**, 590.
3. Brdicka, R. .. *Collection Czechoslov. Chem. Communs.*, 1947, **12**, 212.
4. Delahay, P. .. *J. Am. Chem. Soc.*, 1952, **74**, 3506.
5. ——— and Adams, T. J. .. 1952, **74**, 1436–41.
6. Doss, K. S. G. .. *Proc. Ind. Acad. Sci.*, 1937, **6**, 24.

THE FORCE CONSTANTS OF NITRYL CHLORIDE AND NITRYL FLUORIDE

By Dr. T. A. Hariharan

(*Department of Physics, Indian Institute of Science, Bangalore-3*)

Received January 30, 1958

(Communicated by Prof. R. S. Krishnan, F.A.SC.)

Introduction

Molecules of the type XYZ_2 generally belong either to the point group C_s or to C_{2v}. In the former case the molecule is nonplanar, while in the latter all the four atoms lie in a plane which itself is a plane of symmetry. An investigation of the Raman spectra with the polarisation of the Raman lines will enable one to decide between these two types of symmetry. If the symmetry is C_s there will be four polarised Raman lines, whereas there will be only three polarised lines for symmetry C_{2v}. These considerations have been used by Allen and McDowell (1955) to suggest that the molecule thionyl chloride ($CSCl_2$) is nonplanar and of point group C_s instead of C_{2v} as was assumed earlier by Duchesne (1941, 1954).

A number of investigations on the vibrational and microwave spectra of the compounds nitryl chloride (NO_2Cl) and nitryl fluoride (NO_2F) have been recently reported and the results indicate that the molecules are planar. The infrared spectrum of nitryl chloride in the gaseous state and the Raman spectrum in the liquid state are studied by Ryason and Kent Wilson (1954) and an assignment of the fundamental frequencies has been made. The infrared spectrum of gaseous nitryl fluoride and the Raman spectrum of the liquid at $-95°$ C. are reported by Dodd, Rolfe and Woodward (1956). The microwave spectrum of NO_2Cl has been investigated by Millen and Sinnot (1955). The present investigation deals with the evaluation of the force constants in a valence force potential function using the Wilson's matrix method.

Symmetry Considerations

It is well known that the six fundamental vibrations of a molecule of type XY_2Z (point group C_{2v}) have three vibrations of class A_1, two of class B_1 and one of class B_2. The last one is an out-of-plane vibration and we

shall not consider it here. The symmetry co-ordinates for the planar vibrations are:—

Type A_1:

$$R_1 = \Delta D$$

$$R_2 = \frac{1}{\sqrt{2}}(\Delta d_1 + \Delta d_2)$$

$$R_3 = \frac{1}{\sqrt{6}}(2\Delta\alpha - \Delta\beta_1 - \Delta\beta_2)$$

$$R_4 = \frac{1}{\sqrt{3}}(\Delta\alpha + \Delta\beta_1 + \Delta\beta_2). \qquad \text{(redundant co-ordinate)}$$

Type B_1:

$$R_5 = \frac{1}{\sqrt{2}}(\Delta d_1 - \Delta d_2)$$

$$R_6 = \frac{1}{\sqrt{2}}(\Delta\beta_1 - \Delta\beta_2).$$

Where D, d_i, α and β_i denote the equilibrium values of the distances $X - Z$ and $X - Y_i$ and the angles Y_1XY_2 and Y_iXZ respectively.

Using these symmetry co-ordinates the following G matrix elements can be obtained.

Type A_1:

$$G_{11} = \mu_X + \mu_Z.$$

$$G_{12} = \sqrt{2}\mu_X \cos\beta.$$

$$G_{13} = \frac{2}{\sqrt{6}} p\mu_X \left\{\sin\beta - \left[\frac{2\cos\beta}{\sin\alpha}(1 - \cos\alpha)\right]\right\}.$$

$$G_{22} = \mu_Y + \mu_X(1 + \cos\alpha).$$

$$G_{23} = \frac{2\mu_X}{\sqrt{12}}\left\{\frac{1}{\sin\beta}[2(p - q\cos\beta)\cos\beta + (q - p\cos\beta)(1 + \cos\alpha)] - 2p\sin\alpha\right\}.$$

$$G_{33} = \frac{1}{3}\mu_Y p^2 \left\{5 - \frac{4\cos\beta}{\sin\alpha\sin\beta}(1-\cos\alpha)\right\}$$

$$+ \mu_X \left\{\frac{4}{3}p^2(1-\cos\alpha) + \tfrac{1}{3}\sin^2\beta\,[2(p-q\cos\beta)^2\right.$$

$$+ (q-p\cos\beta)^2(1+\cos\alpha) + 4(p-q\cos\beta)$$

$$\times (q-p\cos\beta)\cos\beta] - \frac{4p}{3\sin\alpha\sin\beta}(1-\cos\alpha)$$

$$\left.\times\,[2(p-q\cos\beta)\cos\beta + (q-p\cos\beta)(1+\cos\alpha)]\right\}.$$

Type B_1:

$$G_{55} = \mu_Y + \mu_X(1-\cos\alpha).$$

$$G_{56} = -\frac{\mu_X}{\sin\beta}(q-p\cos\beta)(1-\cos\alpha).$$

$$G_{66} = \mu_Y p^2 + \frac{\mu_Z q^2}{\sin^2\beta}(1-\cos\alpha) + \frac{\mu_X}{\sin^2\beta}(q-p\cos\beta)^2 \times(1-\cos\alpha).$$

Where μ_i represents the reciprocal of the mass of the atom i, $p = 1/d$ and $q = 1/D$.

The molecular dimensions of the nitryl chloride as given by Millen and Sinnot (*loc. cit.*) are $d(N=0) = 1{\cdot}16$ A. $D(N-Cl) = 1{\cdot}98$ A. $\alpha = 130°$ and $\beta = 115°$. For nitryl fluoride Dodd, *et al.* (*loc. cit.*) have given the dimensions $d(N=0) = 1{\cdot}22$ A, $D(N-F) = 1{\cdot}5$ A, $\alpha = 145$–$155°$. The mean value of 150° has been taken in the present investigation for α and hence $\beta = 105°$. The reciprocal masses of the atoms are $\mu_{Cl} = 1{\cdot}698 \times 10^{22}$; $\mu_F = 3{\cdot}169\times10^{22}$; $\mu_O = 3{\cdot}764\times10^{22}$ and $\mu_N = 4{\cdot}301\times10^{22}$. Using these values the following G matrices have been obtained.

NO_2Cl *Type* A_1:

$$\begin{vmatrix} 5{\cdot}999\times10^{22} & -2{\cdot}57\times10^{22} & 8{\cdot}231\times10^{30} \\ & 5{\cdot}301\times10^{22} & -4{\cdot}92\times10^{30} \\ & & 2{\cdot}414\times10^{39} \end{vmatrix}$$

Type B_1:

$$\begin{vmatrix} 1{\cdot}0829\times10^{23} & -6{\cdot}776\times10^{30} \\ & 1{\cdot}0163\times10^{39} \end{vmatrix}$$

NO_2F *Type* A_1:

$$\begin{vmatrix} 7{\cdot}47\times10^{22} & -1{\cdot}574\times10^{22} & 5{\cdot}558\times10^{30} \\ & 4{\cdot}3403\times10^{22} & -3{\cdot}054\times10^{30} \\ & & 2{\cdot}3756\times10^{39} \end{vmatrix}$$

Type B_1:

$$\begin{vmatrix} 1{\cdot}179\times10^{23} & -7{\cdot}303\times10^{30} \\ & 1{\cdot}199\times10^{39} \end{vmatrix}$$

The potential energy function.—The potential energy function assumed is

$$2V = f_D \Delta D^2 + f_d (\Delta d_1^2 + \Delta d_2^2) + 2f_{dd} \Delta d_1 \Delta d_2 + d^2 f_\alpha \Delta\alpha^2 + d^2 f_\beta (\Delta\beta_1^2 + \Delta\beta_2^2) + 2d^2 f_{\beta\beta} \Delta\beta_1 \Delta\beta_2 + 2d^2 f_{\alpha\beta} \Delta\alpha \times (\Delta\beta_1 + \Delta\beta_2) + 2f_{dD} \Delta D (\Delta d_1 + \Delta d_2).$$

The factored F matrix elements are:

Type A_1:

$$F_{11} = f_D.$$
$$F_{12} = F_{21} = \sqrt{2} f_{dD}.$$
$$F_{13} = F_{31} = 0.$$
$$F_{22} = f_d + f_{dd}.$$
$$F_{23} = F_{32} = 0.$$
$$F_{33} = \tfrac{1}{3} d^2 (2f_\alpha + f_\beta + f_{\beta\beta} - 4f_{\alpha\beta}).$$

Type B_1:

$$F_{55} = f_d - f_{dd}.$$
$$F_{56} = F_{65} = 0.$$
$$F_{66} = d^2 (f_\beta - f_{\beta\beta}).$$

FUNDAMENTAL FREQUENCIES

In the case of NO_2Cl, Ryason and Kent Wilson (*loc. cit.*) have assigned the frequency at 411 cm.$^{-1}$ to the species B_2 and the line 615 cm.$^{-1}$ to the species A_1. But Dodd *et al.* have later suggested that the line 411 cm.$^{-1}$ has to be assigned to the species A_1 and the line 615 cm.$^{-1}$ to the species B_2. The fundamental frequencies and their assignments for the molecules NO_2Cl and NO_2F are given in Table I.

TABLE I

Frequencies in cm.$^{-1}$

Molecule	ν_1 (A_1)	ν_2 (A_1)	ν_3 (A_1)	ν_4 (B_1)	ν_5 (B_1)	ν_6 (B_2)
NO_2Cl ..	1293	794	411	1685	367	651
NO_2F ..	1312	822	460	1793	570	742

Force Constants

The secular equation for the type B_1 vibrations is a quadratic one and hence will yield two values for each of $f_d - f_{dd}$ and $d^2(f_\beta - f_{\beta\beta})$. One of these will not be quite acceptable because it yields a low value of the N=O stretching constant and a high value for the deformation of the angle β. The other solution gives for NO_2Cl, $F_{55} = 8{\cdot}963 \times 10^5$ and $F_{66} = 8{\cdot}378 \times 10^{-12}$ and for NO_2F, $F_{55} = 8{\cdot}82 \times 10^5$ and $F_{66} = 1{\cdot}69 \times 10^{-11}$.

In the case of NO_2F the following combination of the F matrix elements were found to be most satisfactory for the type A_1 frequencies

$$F_{11} = 3{\cdot}516 \times 10^5, \qquad F_{22} = 12{\cdot}9 \times 10^5, \qquad F_{33} = 4{\cdot}303 \times 10^{-12}.$$

These were obtained by giving a series of values to F_{22} starting from $8{\cdot}82 \times 10^5$ and finding out the corresponding values of F_{11} and F_{33} in each case from two equations, namely those for $\lambda_1 + \lambda_2 + \lambda_3$ and $\lambda_1\lambda_2\lambda_3$, where $\lambda_i = 4\pi^2c^2\nu_i^2$. These are then substituted in the equation for $\lambda_1\lambda_2 + \lambda_2\lambda_3 + \lambda_3\lambda_1$ to get the best agreement between the calculated and observed values.

In the case of nitryl chloride, if only the diagonal terms in the F matrix for species A_1 are retained it was found that when F_{22} was increased beyond $10{\cdot}5 \times 10^5$ dynes/cm., the equation did not yield real solutions. Values lower than this is not considered as probable because it will lead to a low value for the force constant corresponding to the stretching of N=O bond. Hence the non-diagonal term F_{12} (or $\sqrt{2}f_{dD}$) was introduced. The most probable values of the constants are then determined in the manner described above and these are $F_{11} = 4{\cdot}19 \times 10^5$; $F_{22} = 10^6$; $F_{12} = 2 \times 10^5$; $F_{33} = 6{\cdot}08 \times 10^{-12}$. F_{22} and F_{55} occur as the sum and difference respectively of f_d and f_{dd} and hence the individual values of f_d and f_{dd} can be easily determined. F_{11} is the value of f_D itself and F_{12} is only $\sqrt{2}f_{dD}$.

Now we have $F_{66} = d^2(f_\beta - f_{\beta\beta})$ and $F_{33} = \frac{1}{3}d^2(2f_\alpha + f_\beta + f_{\beta\beta} - 4f_{\alpha\beta})$. It is not possible with the available data to separate out the individual constants occurring in these combinations unless we make some assumptions. For instance as a first approximation we may neglect the interaction terms $f_{\beta\beta}$ and obtain the value of f_β from F_{66}. In a similar manner we may also neglect the value of the interaction term $f_{\alpha\beta}$ and obtain the value of f_α from F_{33}. The values of the force constants thus obtained are necessarily approximate. It is to be mentioned however that the combinations of the force constants given as elements of the F matrices may be used as such if we want to determine the normal co-ordinates or the transformations between normal

co-ordinates and internal co-ordinates which are required in the intensity problem in infrared and Raman effect.

The individual values of the force constants obtained for NO_2Cl and NO_2F are given in Table II. The force constants are given in 10^5 dynes/cm.

TABLE II

Molecule	f_d	f_{dd}	f_D	f_{dD}	f_α	f_β
NO_2Cl ..	9·48	0·52	4·19	1·41	0·36	0·62
NO_2F ..	10·86	2·04	3·51	..	−0·13	1·13

Even though the molecules NO_2Cl and NO_2F are of similar type, the fundamental frequency of the corresponding linkage N = O as well as the bond length are different in the two cases. This might account for the difference in the values of the calculated force constants.

It can be seen that we are not justified in neglecting the interaction terms $f_{\beta\beta}$ and $f_{\alpha\beta}$ particularly in the case of NO_2F since this leads to a negative value for f_α which is not correct.

In the present investigation we were concerned only with the force constants corresponding to the modes of vibrations confined to the plane of the molecules. The out of plane vibrations are not considered because they require different symmetry co-ordinates and potential function, and this investigation using a slightly modified method is under progress.

The author wishes to express his grateful thanks to Professor R. S. Krishnan for his kind encouragement and interest.

SUMMARY

The force constants of two molecules, nitryl chloride and nitryl fluoride have been calculated using the Wilson's matrix method for a valence force potential function. Only the frequencies of the inplane vibrations have been considered.

REFERENCES

1. Allen and McDowel .. *J. Chem. Phys.*, 1955, **23**, 209.
2. Duchesne .. *Physica*, 1941, **8**, 525.
3. ——— .. *J. Chem. Phys.*, 1954, **22**, 1464.
4. Ryason and Kent Wilson .. *Ibid.*, 1954, **22**, 2000.
5. Dodd Rolfe and Woodward *Trans. Faraday Soc.*, 1956, **52**, 145.
6. Millen and Sinnot .. *Chem. and Ind.*, 1955, 538.
7. Smith and Magnuson .. *Phys. Rev.*, 1952, **87**, 226 A.

708-58. Printed at The Bangalore Press, Bangalore City, by C. Vasudeva Rao, Superintendent and Published by The Indian Academy of Sciences, Bangalore.

NOTICE TO AUTHORS

Scientific papers intended for publication in the *Proceedings of the Indian Academy of Sciences* can be accepted only when they are communicated by a Fellow of the Academy whose duty shall be to satisfy himself that such communications are fit to be read at the Meeting of the Academy and published in its *Proceedings*.

Papers should not ordinarily exceed fifty pages of foolscap. MSS. should be either typewritten or written in legible hand on one side of the paper. All papers should be carefully revised by the authors and should be absolutely in final form for printing. Position for text-figures should be indicated. Each paper shall conclude with a critical summary not exceeding 350 words.

Drawings, diagrams or other illustrations should be made on larger scale (preferably) twice the size than the ones in which they are intended to appear. They should be done in Indian ink on bristol board with lettering in pencil. Scale of magnification of camera lucida tracings should be indicated by the side of drawings. In certain special cases arrangements will also be made for monochrome lithographic and other colour plates. Reduction of illustrations desired should be indicated in pencil. Appropriate legends should accompany all drawings. Names of authors are to be marked in pencil on the left-hand corner of drawing sheets. Photomicrographs should be securely mounted with colourless paste.

All tables, quotations and footnotes which will be set hereafter (beginning from Vol. I, No. 2) in types smaller than the text, should be typewritten on separate sheets and placed with the text in proper sequence. Footnotes should be numbered in Arabic numerals.

References to literature in the text should be given, whenever possible, in chronological order, only the names of authors and years of publication, in brackets, being given. They should be cited in full after the summary, the authors' names following in alphabetical order. Thus,

Name or Names of author; Name of Journal (abbreviation) with a single underline; Year of publication; Number of Volume with a double underline, and lastly page. The following would be a useful illustration:—

Bergmann and Stather . . . . . Z. Physiol. Chem., 1926, 152, 189.

Two copies of slip-proof and wherever possible, a page proof for final revision will be sent to authors. All corrections are best made on the slip-proof which should be transmitted to the Office of the Academy. All proof corrections involve heavy expenses which would be negligible if the papers are carefully revised by the authors before submission.

Fifty free reprints including plates and with cover will be supplied for each paper. Additional copies can be supplied at cost on previous intimation.

Blocks appearing in the *Proceedings* will be available for purchase by their respective authors. Orders for the same should be sent along with the corrected proofs and in any case not later than one month after the date of publication of the paper. The price charged would be 25% of the actual cost of the blocks *plus* freight and despatching charges. If the blocks are reproduced in other journals or publications, due acknowledgment should be made in them to the *Proceedings*.

The original drawings and plates of blocks appearing in the *Proceedings* will be returned to such of the authors as may require them provided the cost of despatching such originals is borne by them.

CONTENTS

PAGE

The Diffraction of X-Rays by Diamond: Part III . . . Sir C. V. Raman 1

Clinohumite Sausar Series, Bhandara District, India . . T. N. Muthuswami 9

Studies on the Relation between Chemical Constitution and Ultraviolet Absorption Spectra of Optically Active and Racemic Compounds. Part VII. Correlation of Absorption Maxima, λ_{max} and Characteristic Wavelengths, λ_{ch}, of Camphor-β-Sulphonyl-phenyl, -tolyl (*o*-, *m*- and *p*-) and Naphthyl (α- and β-)-amides . . . . . Bawa Kartar Singh and Shiva Mohan Verma 29

Polarographic Reduction of Pyruvic Acid . . . . . K. S. G. Doss and (Mrs.) Sarada Menon 43

The Force Constants of Nitryl Chloride and Nitryl Fluoride . . . . . Dr. T. A. Hariharan 49

C